The Feasibility of Producing an MR Damper for Use On a Formula SAE Car

by

Devin E. Norton

A thesis submitted to the Department of Mechanical Engineering
in the Graduate School of Bradley University in
partial fulfillment of the requirements for the Master
of Science degree.

Peoria, Illinois

December 4, 2013

This Thesis for the M. S. Degree

By

Devin E. Norton

has been approved

December 4, 2013

_____

Dr. Julie Reyer, Thesis Committee/Chair

_____

Dr. John Engdahl, Thesis Committee

_____

Dr. Richard Johnson, Thesis Committee

_____

Dr. Desh Paul Mehta, Dept. of Mechanical Engineering

Abstract

Increased interest in Magnetorheological (MR) suspension technology has brought continued research into certain areas such as: control strategies, damper designs, and suspension models. Although more research has been performed, producing a controllable damper out of a commercially available passive damper has not been proven to be feasible for use on a Formula SAE car. A prototype MR damper was proposed and fabricated for use in evaluating the feasibility of the system. Different qualities such as damping range, durability, hysteresis, and plastic deformation of the MR fluid in the damper will be evaluated using a shock dynamometer. The MR damper will be installed on a Formula SAE car to determine its benefits while cornering.

The average lateral acceleration during a sustained right corner for different current levels will be determined, and the standard deviation from that average will be found. With this information, the severity of corrections made to the car will be evaluated to supplement the driver feedback that was collected after testing. The results from all the forms of testing will be compared to validate the MR damper on the basis of design, repeatability, and benefits to the vehicle dynamics of the car.

The proposed MR damper system, if pursued further, could be developed to replace the passive dampers currently being used on the most Formula SAE cars. Recommendations are made to steer future research into the areas that the current research didn't develop. A pair of MR dampers with a semi-active controller was recommended for implementation in future development work.

Acknowledgements

I would like to the my advisor, Dr. Julie Reyer, for her continued encouragement and guidance throughout my time as an Undergraduate and Master's student in the Mechanical Engineering Department. I am forever grateful to Mr. Sandy Moldovan for his words of wisdom throughout my life; For without his encouragement and support I wouldn't have considering pursuing graduate school in the first place. I would also like to thank Dr. John Engdahl and Dr. Richard Johnson for agreeing to serve on my thesis committee. I am thankful to Prof. Steven Gutschlag and Dr. Kelly Roos for their continued help throughout the course of my thesis. I am also very thankful to Dr. José Sánchez and Dr. Ronald Jetton for their guidance and support throughout my education at Bradley University.

I would like to thank my close friend and classmate, Jon Kellogg, for his unwavering help in the fabrication, installation, testing, and review stages of my thesis. I would also like to thank my best and closest friends: Josh Shirk, David Kraus, Corey Burklund, Paige Burklund, and Nate Macnider for their endless support and encouragement throughout my Undergraduate and Master's work; Their friendship made this long journey much easier to bear. Also I would like to thank my close friend, Alyssa Macuk, for her support; Without her weekly discussions, this endeavor would have been even harder. I am thankful to my friend and classmate, Troy Ament, for his help and insight throughout my thesis. I am also thankful to my peers: Greg Heinlein, Matt Bunten, Jim O'Connor, and Jay Anderson for their camaraderie and support throughout my time as a Master's student.

Finally and most importantly, I would like to thank my family for all of their love and support. I would especially like to thank my parents for their love, care, encouragement, guidance, wisdom, and financial support throughout my entire life; Their support is what kept me going through all of the tough times that I encountered along the way. Without them none of this would have been remotely possible.

Table of Contents

Chapter 1: Introduction, Background, and Problem Statement

Introduction

A vehicle suspension is comprised of two major components: a spring and a damper. Each of these components plays their role in suspending the body of the car above the wheels. On a road vehicle, there are four springs and four dampers being used, one of each is installed on each of the four wheels on the car. The springs support the static weight of the vehicle and also set the height of the body off the ground. The dampers help control the weight transfer of the vehicle as well as absorb the forces that are seen by the wheels. In addition, the springs help the damper dissipate the forces and bring it back to its neutral position after the forces have been dissipated. While both of these components are important in determining how the vehicle reacts to changing road conditions, only the dampers will be studied in this thesis.

A suspension damper is made up of a number of components. The main components consist of the shock tube, the piston, the piston rod, and rod end. The shock tube houses most of the other components and the damping fluid. To tie the movement that the suspension has to the damper, the rod end is attached to both the suspension arms and the damper's piston rod. The piston rod is attached between the piston and the rod end to actuate the piston as the suspension moves. To help dampen the suspension forces, the piston moves through the fluid that is inside the damper. As the piston is actuated due to changing road conditions, the fluid inside the damper resists flowing through the piston's orifices. Therefore, the piston decelerates due to the resistance force of the fluid. For a given damper piston velocity, a certain resistance force is

generated by the fluid to counteract that piston velocity. Combined, these components are used to dampen vibrations in the suspension system.

The most common damper type is a passive style damper, which is used in most production cars today. The passive dampers used in passenger vehicles work to damp the forces that are transmitted through the tires, while giving a comfortable ride. For a passive damper to give a comfortable ride to the occupants, compromises to the absorption qualities must be made. Passive suspensions don't have the ability to produce favorable results in both ride control and ride quality. The ride quality must be sacrificed in order for the damper to keep the car more rigid. By compromising between ride quality and road holding, both aspects fail to function well.

For a racing application, it is more important to reduce body roll and ride height changes rather than maintaining a comfortable ride. Transferring too much weight from certain tires can cause the vehicle to become unstable. Which is why reducing body roll and ride height changes are so important. Every suspension scenario has different damping needs. Therefore, compromises still exist even when ride control is the more important design aspect of the car. Usually the damper has to be setup to work best during a specific type of corner, while compromising some of its performance in others. This additional compromise makes it more difficult to use all of the vehicles potential while cornering.

Controllable dampers attempt to alleviate the compromises associated with passive dampers by allowing the damping to change from corner to corner. Controllable suspension dampers allow the weight transfer to be controlled more precisely, which allows the vehicle and driver to maintain control in any situation. This type of damper can be set up to control the

suspension for a comfortable ride or road holding, depending on the desired application. They can even be set up to do both of these at different times, depending on the road conditions.

Since the system is set up to control the suspension on a situational basis, fewer compromises have to be made between ride comfort and road holding. Racing applications can benefit from the advantages of the ability to fine tune the damping for the corner at hand. These advantages are even more important when the competitors are closely matched. The Formula SAE competition has always been a closely attested student design and racing event. Teams from all over the world have been trying to find the smallest edge to push their cars into the winner's circle. One aspect of the car that hasn't been significantly changed throughout the years is the suspension.

Although different ways of building the suspension have been tried, very few changes to the dampers have been made. A few teams have installed MR dampers on their cars, but overall the majority of teams are still using passive dampers. Yet, some automotive manufacturers are starting to incorporate MR dampers into the vehicles. However, there are reason why MR dampers are not being widely developed and used in the Formula SAE competition. The biggest of these reasons are: cost, packaging, complexity, and fabrication. However if these barriers can be overcome, the cornering ability of the car can be greatly improved. This improvement thus gives a team an advantage in the competition.

This thesis will look to determine the feasibility of creating an MR damper out of a passive damper and implementing it on a Formula SAE car. Existing controllable damper designs will be shown and compared to one another. Also the properties of MR fluid will be explained, in order to give a background for the MR damper design process. Without

background knowledge in the suspension models that explain how a damper affects the suspension dynamics, an MR damper cannot be properly designed. For this reason, background information is also presented on different suspension models. Since semi-active control is what governs the performance of any MR damper, feasible control strategies play a deciding role in the overall design. The background information presented explains why different design decisions were made.

There are a number of different components that make up an MR damper. Each component has to be specifically chosen in order to turn a passive damper into a semi-active one. The biggest component of an MR damper is the fluid inside it. Once MR fluid has been chosen for the damper, more decisions can be made. The theory governing MR fluids is shown to present these different decisions that must be made in order to determine the proper MR fluid for the given application. To create a magnetic field within the MR damper, a magnetic coil needs to be developed and created. The concepts and equations that govern a magnetic coil are given to backup the design decisions that were made.

A prototype MR damper that can be used on the 2013 Bradley University Formula SAE car. A number of different aspects of the damper will be tested before the feasibility can be determined. A current limit will be established for the magnetic coil, and the system will be tested at different current levels to determine the different damping curves that can be created. The results from this test are shown and interpreted in this thesis. Along with the different damping curves that can be created, the variation between cycles plays a key role in overall performance of the MR damper. The tests to determine the variability of the MR damper are explained along with the results from these tests. After the overall performance of the MR damper was determined on a damper dynamometer, a durability test was needed. The results

from running this test are shown, which explain how the magnetic coil would react to a high current being applied for an extended period of time. The MR damper will also be tested on a Formula SAE car to determine if different settings produce a difference in handling and controllability. These different aspects will allow the MR damper design to be validated and also help to determine whether or not it is feasible to produce a semi-active Formula SAE suspension using a commercially available passive damper.

Background

Controllable Damper Designs

Research into active and semi-active suspensions has become prevalent in recent years since they lend themselves to being used in applications where compromises in the suspension dynamics must be limited. While active suspensions require a much bigger financial investment in order to be developed, they allow for the suspension to be truly controlled in an active manner, changing the dynamics of the suspension system entirely. The main type of active damper is a force actuator. A force actuator can't be used in events such as Formula SAE. This is due to the rules requiring the use of a suspension damper, which makes it impractical to study in this thesis. Semi-active suspensions on the other hand, require a much smaller investment due to the increase in their research and development. Another quality that make semi-active suspension dampers desirable is that they maintain the same basic dynamics of a passive suspension system. In the simplest form, a semi-active suspension is comprised of a spring and a controllable damper. A controllable damper does not possess truly active characteristics because they react to

a change in either the road or damper behavior. There are two main types of controllable dampers: frictional dampers and controllable fluid dampers.

Friction force dampers are more unconventional in automotive applications than controllable fluid methods. In a friction force damper the force applied to the piston is dissipated through the regulation of fluid within the damper. The damper must have the capability of being controlled in a logical fashion. The common way of accomplishing this is to use an electrohydraulic drive to control the hydraulic pressure in the damper. This can be done by using a pump and a servo valve in parallel to change and regulate the pressure pushing against the piston (Guglielmino et al. 2008). This type of damper can be seen in **Figure 1**. Although this method works well for one damper, as you begin to complicate the system and add more dampers it becomes unpractical.

In order to control multiple dampers the system would need the same number of pumps and valves as dampers. An alternative to this is to use a three-way proportional flow control underlapped valve to control the pressure driving a single-chamber actuator (Guglielmino et al. 2008). This allows for one pump to feed the entire system as shown in **Figure 2**. Friction force dampers add more weight to the system because they have more components as well as needing a separate tank for the extra fluid to be stored in. This added weight is detrimental to the performance of a racing vehicle. In addition, the extra components take up space in the vehicle that make them undesirable for applications where space is a concern. The aforementioned qualities make frictional dampers less desirable to use in automotive applications than other semi-active options.

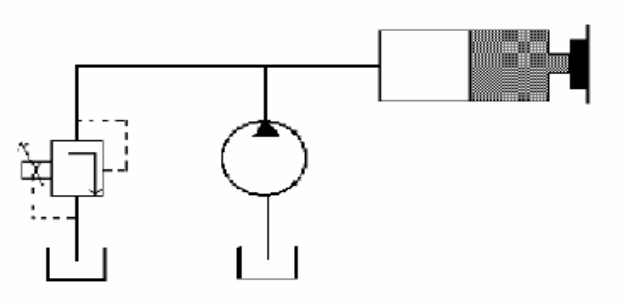

Figure 1: Friction Force Damper w/ Electrohydraulic Drive (Guglielmino et al. 2008)

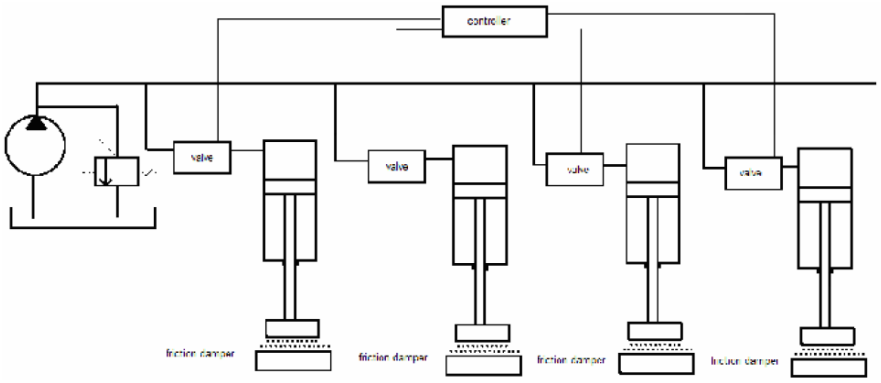

Figure 2: Independent Flow Control Setup (Guglielmino et al. 2008)

The most common type of controllable dampers used in automotive applications is the controllable fluid damper. A controllable fluid damper attempts to alleviate the compromises of a passive damper by using fluid that can be changed depending on the situation. By using a set of sensor to determine the velocity of the piston, a controller changes the current and voltage in the system. This change in current and voltage affects the fluid inside damper, causing the fluid to change its microstructure. The change in microstructure affects the effective viscosity of the fluid, causing the damping force associated with a specific velocity to change accordingly. These qualities make a controllable fluid damper ideal for use in automotive applications.

There are a few different types of fluid that can be used in a controllable damper for automotive applications. By far the most prevalent in recent automotive applications is

Magnetorheological (MR) fluid. MR fluid uses non-colloidal suspended ferrous particles that are only a few microns in size. These particles in the case of dampers are suspended in damper oil. The application of a magnetic field can rapidly change the rheological behavior of an MR fluid. In the absence of a magnetic field the MR fluid behaves similar to a standard oil. As the current that is feeding the magnetic field changes, the viscosity within the MR fluid also changes (Guglielmino et al. 2008). This gives the MR damper a high degree of controllability without adding a substantial amount of weight to the system. Compared to other controllable fluids, MR fluid requires a small amount of power which make them easy to incorporate into a vehicle. MR fluids also require a small response time to change from state to state. In some tests, MR fluid has responded to changes in field strength in under 10 milliseconds. These properties make MR fluids desirable for use in automotive applications.

There are three main MR damper designs: monotube, twintube, and double ended, that are currently being used in applications where damping is required. Monotube dampers are by far the most common of the three types. Due to their compact size they can be mounted in tighter areas than the other designs. Also, because they only have one fluid reservoir and a gas accumulator, they can be mounted in any orientation. The gas accumulator is included to account for the increase in volume as the piston shaft moves into the damper body (Poynor 2001). In some cases, there is also an extra fixed piston just below the accumulator that further affects the dynamics of the flowing fluid. With this added benefit, the damper has more adjustability. **Figure 3** shows the basic setup of a monotube MR damper.

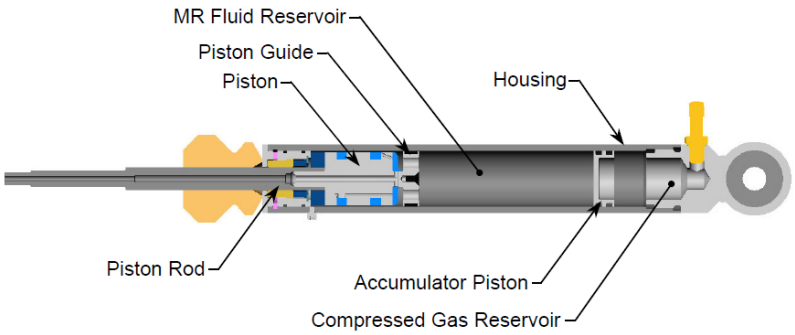

Figure 3: Basic Monotube MR Damper Setup (Poynor 2001)

The second most common MR damper design is the twintube MR damper. Instead of having a single fluid reservoir and a gas accumulator, it has two separate fluid reservoirs. By having two separate reservoirs, the gas accumulator is removed which allows for the damper to be shorter. Although it is shorter, it has a larger diameter because of the two concentric reserviors. The outer reservoir is not completely filled with fluid which causes variability to arise without careful measuring of the volume. By changing the amount of fluid in the outer reservoir of the damper, the forces for a given velocity change, which gives it an added area for fine tuning. The outer reservoir also serves the same purpose as the gas accumulator in the monotube shock. By moving fluid to the partially filled outer reservoir, the volume change as the piston rod moves into the damper body is taken into account (Poynor 2001). The material weight is greater than a monotube damper because it has to have two separate housings. This added weight makes it a less desirable choice when weight is a strong concern. The basic setup for the twintube MR damper is shown in **Figure 4**.

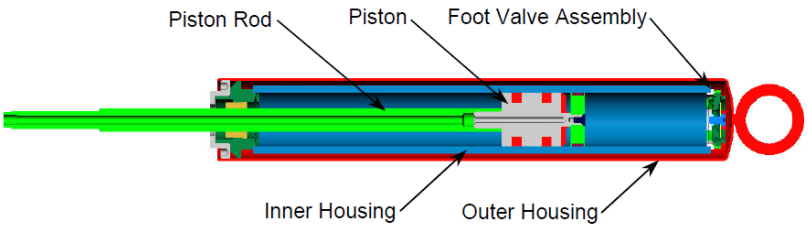

Figure 4: Basic Twintube MR Damper Setup (Poynor 2001)

The third common MR damper design is a double-ended MR damper. This design uses two pistons and piston rods that oppose each other. In this design, as the pistons move the volume doesn't change. This is accomplished by having the piston rods the same diameter (Poynor 2001). **Figure 5** shows the general setup of a double-ended MR damper. As can be seen in the figure, the double-ended MR damper doesn't lend itself well to an automotive application. This is because both pistons must be able to move for the system to work. These MR dampers represent the main types that can be produced, but only two of them can be easily applied to automotive applications.

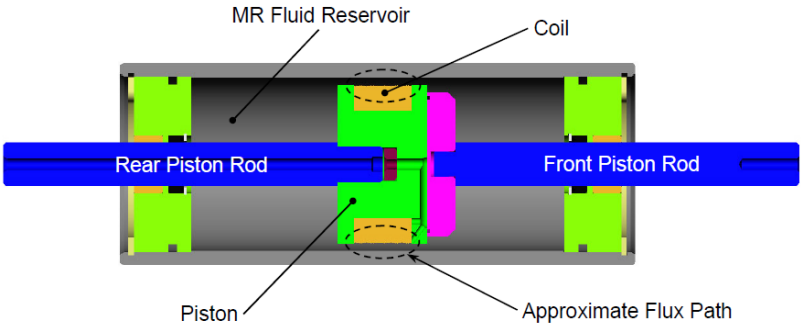

Figure 5: Basic Double-ended MR Damper Setup (Poynor 2001)

Two different magnetic coil designs: an internal coil and an external coil, have been found to be effective in creating the magnetic field required for the MR damper. An external coil

such as the one in **Figure 6** is one option for placing the magnetic coil. This design uses a magnetic coil that is fixed to the outside of the monotube damper. The magnetic coil can be bigger because the only size limitation is other components around the damper. With this design the initial field strength needs to be higher because the field has to permeate through the damper tube before reaching the MR fluid.

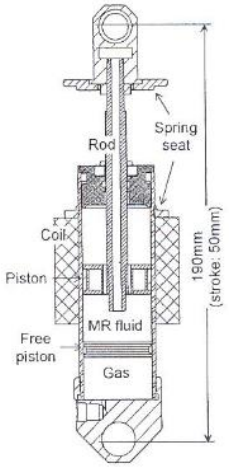

Figure 6: MR Damper w/ an External Coil (Komatsuzaki et al. 2007)

The other main option for an MR damper is an internal coil design like that of **Figure 7**. The magnetic coil is housed inside the monotube damper with the wires running through the shock rod. Usually the coil is placed inside the piston but could be located in a few different locations around the inside of the damper. In this type of design the coil moves with the piston creating a relatively constant field strength at any point along the stroke length. The coil size is smaller due to the need for a smaller magnetic field localized at the piston. The issue with this lies in the size constraint of the coil; It is restricted to the space that can be used inside the piston.

In Komatsuzaki's et al. SAE technical paper the development of an MR damper was briefly discussed for an off road application. Both internal and external coil designs were tested

and the internal coil was eventually developed further. The internal coil design was further developed because the external coil design didn't produced enough of a change in the relative damping coefficient when the current was varied from 0 amps to 2 amps (Komatsuzaki et al. 2007). The two main designs for the magnetic coil differ greatly from one another, but both provide viable options for producing a magnetic field as long as they meet the requirements.

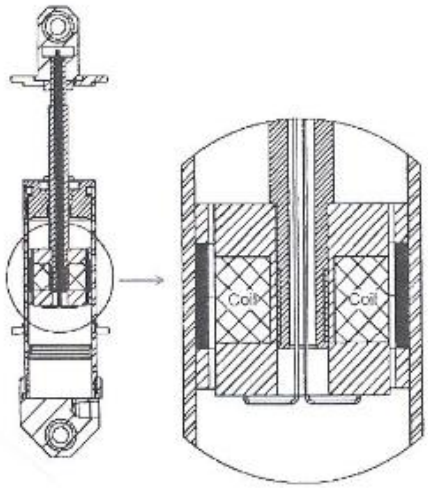

Figure 7: MR Damper w/ an Internal Coil (Komatsuzaki et al. 2007)

Installing the coil inside the piston is a challenge because the size of the piston is so small that it makes it difficult to find enough room to put the coil and the fluid passages. Even for an external coil design it can be a challenge because the coil has to be big enough to produce the required magnetic field strength, while also being small enough to fit in tighter locations. Also, the increases in damping force have not been shown to outweigh the extra cost and weight that is associated with MR dampers. The MR fluid requires a certain amount of magnetic field strength to produce certain damping forces even in small quantities. Therefore, in order for a small damper to produce a damping force significantly higher than its original one, a relatively large magnetic coil must be used. A magnetic coil of this size can increase the weight of the small

damper immensely, causing them to be less desirable for these types of applications. These aspects have caused the development of small application MR dampers to suffer up to this point.

MR Damper Usage in Formula SAE

As was briefly discussed above, MR dampers have not been used by many teams in the Formula SAE competition. Lawrence Technological University developed an MR damper that they tested on their Formula SAE car for use in the 2001 Formula SAE competition (Jawad 2001 & 2002). They placed 12th and 10th for the skidpad and autocross events, respectively, in the 2001 Michigan Formula SAE competition (Formula Student Germany 2013). Lawrence found that the MR damper was a great advantage in controlling the roll of the car during cornering maneuvers at various speeds (Jawad 2001 & 2002). Kanazawa University developed an MR damper for use in their 2007 Formula SAE car (Komatsuzaki et al. 2007). They placed 23rd in autocross in the 2007 Student Formula SAE Competition of Japan. They did not complete the skidpad event for the competition (Formula Student Germany 2013). Kanazawa found that the MR damper benefited the cars cornering over their passive damper design from the previous year (Komatsuzaki et al. 2007). The University of Toronto is currently using MR dampers on their Formula SAE car (Kasprzak 2012). Toronto has used MR dampers on their Formula SAE car for the 2012 Formula Student Germany competition (Bakaic 2012). They finished 54th in the skidpad event and didn't complete the autocross event (Formula Student Germany 2013).

Testing Platform

The testing platform for this thesis will be the 2013 Bradley University Formula SAE car. The 2013 car has a motion ratio of 1:1 with Short-Long suspension arms (SLA). It has four AFCO Series 51 Quarter Midget dampers that utilize a 3:1 rebound damping bias. Each damper has a 165 pounds per inch spring attached to it; The front springs have two and a half turns of preload and the rear springs have one turn of preload.

MR Fluid Properties

MR fluids have many distinct properties that make them different from other fluids that are used in damper applications. These properties make it desirable from a controllability aspect because they allow the fluid to be changed to meet the changing situational requirements. Although they have distinct properties from other damping fluids, they do share some of the same qualities. These distinct property differences are what make MR fluids different and more complex to work with than other damping fluids.

When a magnetic field is present, the area of fluid that is within the magnetic field acts like a semi-solid. This happens because the ferrous iron particles in the fluid align themselves in chains along the magnetic flux lines as in **Figure 8**. These chains resist movement away from their magnetic flux lines (Poynor 2001). This resistance is called the effective yield stress of the MR fluid. As the magnetic field strength increases, so too does the effective yield strength of the material. The yield strength increases the force that is exerted on the piston to counteract its velocity.

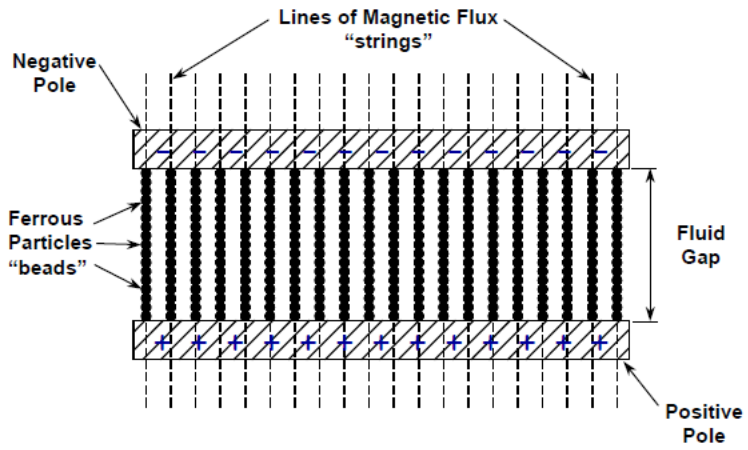

Figure 8: Ferrous Iron Particles Alignment Characteristics (Poynor 2001)

The ferrous iron particle chains also act in a way that restricts the flow of fluid through the piston. This restriction further increases the damping force. Although the force increases with velocity, there is a point where the semi-solid starts to plastically deform under a given magnetic field strength. MR fluids act in a Bingham-plastic like behavior (Li et al. 1999). A Bingham-plastic material acts like a solid at low stresses and a viscous liquid at high stresses. This causes the material to have defined viscoelastic and viscoplastic regions. Even though MR fluids exhibit similar qualities to that of an ideal Bingham-plastic model, they do not act in an ideal manner (Li et al. 1999). **Figure 9** shows that the effective yield stress changes nonlinearly as the current increases. The damper yield force shown in the figure represents the effective yield stress of the MR fluid in terms of the force required for the damper's piston to yield the fluid. This nonlinearity comes from the magnetic field strength starting to saturate within the coil (Reader 2009).

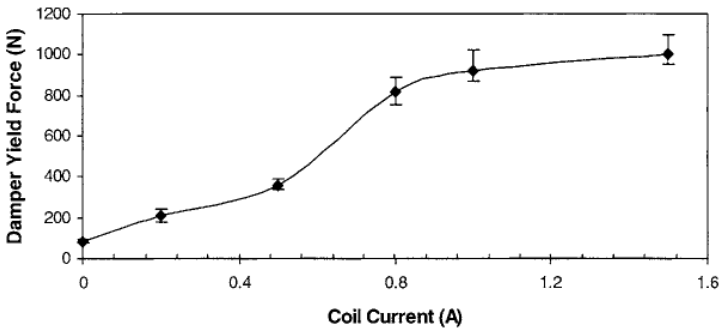

Figure 9: Idealized Yield Stress vs. Magnetic Coil Current (Li et al. 1999)

Another phenomenon that can occur in MR fluids is hysteresis. The variance and gap that develops between the two halves of the compression or rebound stroke is what is known as hysteresis. It occurs when the damper switches acceleration directions while the velocity is still in the original direction. Hysteresis greatly affects how a damper reacts to positive and negative accelerations of the piston. It effectively changes the damping curve for a period of time until it subsides. Hysteresis occurs when the fluid velocity and the piston velocity are in the same direction, but the residual forces acting on the piston have a greater magnitude. This produces more force at a given velocity until the fluid velocity again equals the piston velocity. MR fluid starts to develop hysteresis as the current increases as shown in **Figure 10**.

As this occurs, the transition point from compression to rebound changes. In a passive damper, the transition point is at zero when the damper is tuned properly. In an MR damper on the other hand, as the current increases the transition point moves upward. Although hysteresis changes the damping value, it can easily be accounted for in the controller. Hysteresis develops when the velocity of the damper starts to decrease, which causes variance. These variations in the damping curve affect the overall performance of the damper, but can be accounted for through the use of an active controller.

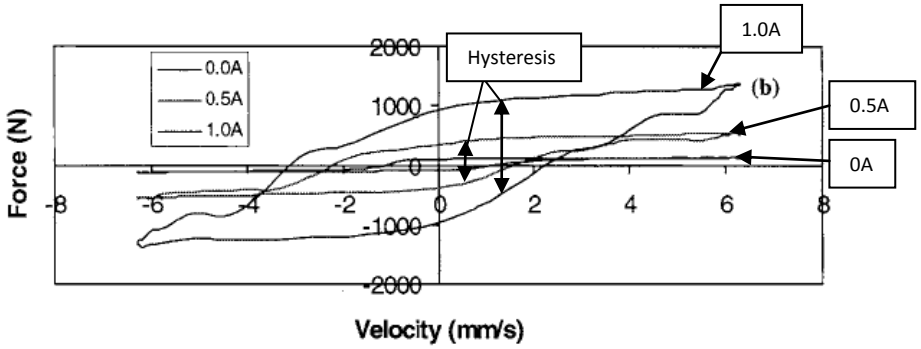

Figure 10: Idealized Hysteresis at Different Current Levels (Li et al. 1999)

There has been research in developing a model to depict the hysteresis behavior of MR fluid. More specifically, research has been dedicated to the development of an MR damper model which incorporates the Bouc-Wen hysteresis model. The Bouc-Wen hysteresis model works well to predict the behavior of hysteretic materials. By adjusting some of the parameters in the damper model, different aspects of the force versus displacement curve can be changed. Aspects such as the linearity in the unloading portion of the cycle and also the transition smoothness from the pre-yield to post-yield region can be controlled. The original MR damper model that incorporates Bouc-Wen hysteresis effects is shown in **Figure 11**. Although the original damper model resembles how an MR damper behaves, the nonlinear force versus velocity response does not accurately portray the roll-off that occurs when the velocity and acceleration have opposite signs (Spencer Jr. et al. 1997).

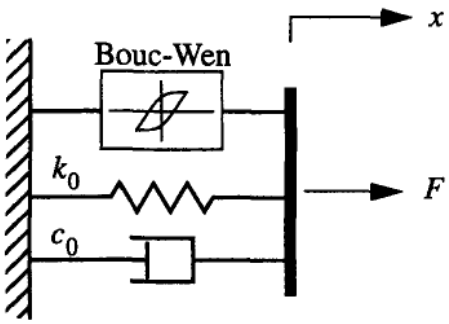

Figure 11: Original MR Damper Model Incorporating Bouc-Wen Hysteresis Effects (Spencer Jr. et al. 1997)

To incorporate this area, a modified version of the MR damper model was proposed. This modified version is shown in **Figure 12**. The modified model contains two more elements that account for aspects of the MR damper cycle that were not included in the original MR damper model. The extra spring, k_1, represents the accumulator stiffness that is present in a monotube damper with a gas accumulator. The second element that was incorporated into the modified model was a second damping force, c_1. The second damping force accounts for the roll-off in lower velocities ($\leq$ 2 in/sec) that was previously excluded from the model. The first damping force, c_0, in the modified model refers to the viscous damping that occurs at larger velocities (> 2 in/sec) (Spencer Jr. et al. 1997). With these added elements, the Modified MR damper model more closely represents the force versus velocity behavior of an MR damper.

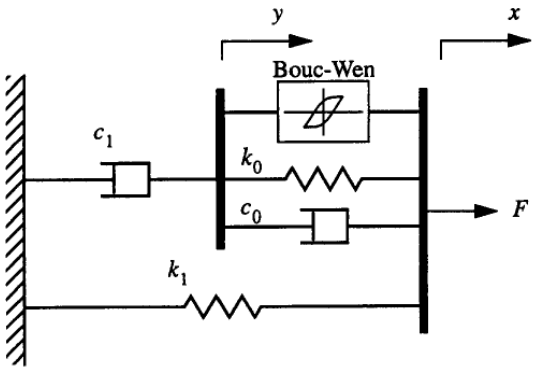

Figure 12: Modified MR Damper Model Incorporating Bouc-Wen Hysteresis Effects (Spencer Jr. et al. 1997)

Suspension Control Strategies

In order for a semi-active suspension to work properly it has to be controlled in some manner. There are a number of different control strategies that can be employed to accomplish this. These strategies can be summed up into two categories: predictive and feedback control. In addition to these, a number of different suspension control techniques can be used to produce the desired ride of the vehicle for either type of control strategy. Predictive control uses sensors placed on the front of the vehicle to determine the road conditions ahead of it. The sensors determine what is coming up on the road surface to give the controller information to determine what changes need to be made to the damper's viscosity. Feedback control on the other hand uses sensors to determine what the car is experiencing at that instant. This data again is fed to the controller to determine the course of action for changing the damper's viscosity (Marzbanrad et al. 2012). These control types represent how the controller collects information for use in the control strategy of the MR damper.

Different damper control strategies have been developed over the years to minimize acceleration of the sprung mass. By controlling the acceleration of the sprung mass for each corner of the vehicle individually, a precise weight transfer rate can be achieved. The controller uses the information that was collected from the sensors to determine what kind of damping rate is needed to achieve a specific rate of weight transfer. A number of different control strategies help to maintain the grip to all of the wheels throughout a maneuver: balance, skyhook, and groundhook control logic (Zhang et al. 2013).

Balance control logic aims at reducing the overall acceleration of the sprung mass. By using relative displacement and velocity of the sprung mass procured from a set of sensors, the damping force can be modified in a sequence of changes within the bounds of the fluid characteristics to achieve the damping force. This method of control works well when you want to balance the weight of the car between the four dampers evenly. When the car is cornering though, having the weight balanced evenly between the dampers doesn't allow for good grip to the tires that need it most. Balance control logic aims to reduce the acceleration by balancing the weight but doesn't allow for more weight to be given to certain tires when needed (Zhang et al. 2013).

Skyhook logic is another control strategy that uses sensor readings for either displacement or velocity to control the acceleration of the sprung mass. The skyhook control logic is described as suppressing the sprung mass acceleration by increasing and decreasing the viscosity of the fluid. The big difference between balance and skyhook logics is that skyhook uses an ideal fixed point in the sky that the damper is hooked to. This limits the driving factor to only the sprung mass velocity (Zhang et al. 2013). The skyhook type of logic excels at isolating the sprung mass of the vehicle. As can be seen in **Figure 13** though, the skyhook technique does

not help reduce the displacement of the unsprung mass of the vehicle. This can cause the displacement of the unsprung mass to increase due to different damping characteristics (Blanchard 2003). This form of control logic does allow for more weight to be transferred to certain tires when they need it, but is more complex to program than other forms of control logic.

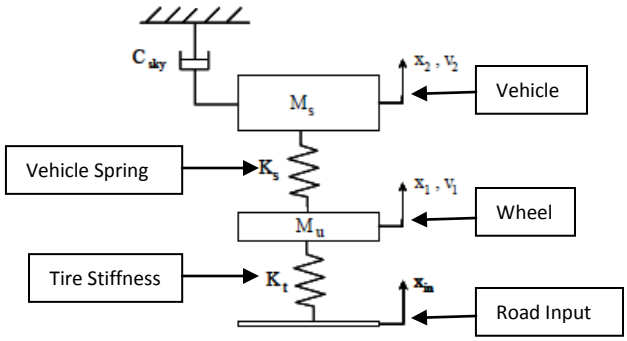

Figure 13: Skyhook Control Logic Model [Blanchard 2003]

The third major control strategy is groundhook logic. This technique is very similar to the skyhook logic. It uses the same techniques and strategies to control the viscosity, but instead of using an ideal fixed point in the sky it uses the ground for the fixed point. Instead of being connected to the sprung mass, this fixed point is connected to the unsprung mass. This method has the same type of issues as the skyhook method but the roles are reversed. In **Figure 14**, the sprung mass is more likely to have an increased displacement and the unsprung mass is more isolated from the excitations (Blanchard 2003). Groundhook control logic aims to keep high adhesion between the tire and the road surface while leaving the sprung mass to move more freely. This type of control logic also works well for automotive applications, but it too requires more programming and computer power to use than other forms of control logic.

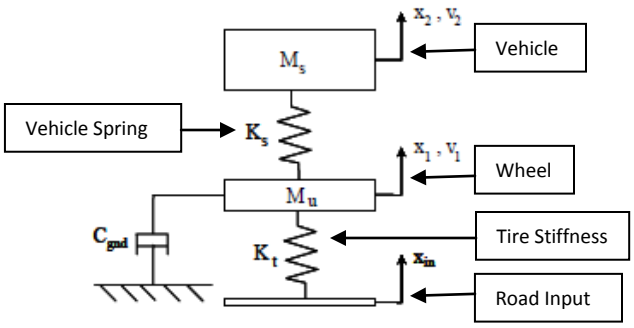

Figure 14: Groundhook Control Logic Model (Blanchard 2003)

Problem Statement

The purpose of this thesis is to determine the feasibility of creating an MR damper for use in a Formula SAE Car using a commercially available passive damper. This concept, however, has not been studied in-depth for use in a Formula SAE Car. This thesis will detail the design process for retrofitting MR damper technology into a commercial passive damper, determining its feasibility through testing on a damper dynamometer, and adaption to a Formula SAE car.

Chapter 2: MR Damper Design

The different components that make up an MR damper will be explored in the section. Since there are different kinds of MR fluid, the proper one needs to be determined for the application. The different kinds will be evaluated and the MR fluid that best fits the application's requirements will be determined. The magnetic coil plays a big role in the MR damper design. The field strength for the application will be shown and from that the current and number of turns for the application will be determined. There are also different ways that the MR damper body can be designed. Either a passive damper can be used as a starting point or a completely new design can be created. For use in this thesis, an AFCO 51 Series Monotube Quarter Midget damper will be used as the starting point. The AFCO damper was chosen because it is currently being used on the 2013 Bradley University Formula SAE car.

Not only does the damper body have these choices, but the components inside the damper body do too. The damper body and its inner components will be evaluated to determine which route is the proper one for this thesis. The placement of the magnetic coil determines how the field interacts with the MR fluid. Different placements of the coil will be considered and the one that best meets the requirements of the design will be determined. Depending on the placement of the magnetic coil, it also has to be attached to the rest of the MR damper. Different attachment options will be considered for the chosen placement of the magnetic coil. Once the new components have been designed, an FEA will be performed to evaluate their factors of safety against failure.

MR Fluid Theory

The fluid inside the shock is one of the key components that makes an MR damper different from a passive damper. MR fluid is made up of a carrier fluid that is formulated to suspend the magnetic particles inside it. For the specific MR fluid being considered, the magnetic particles are made of soft iron and are roughly 6μm in size. It was produced by the Lord Corporation, which produces three different types of MR fluid. The main difference between the three types is the viscosity of the fluid under no magnetic field. The typical fluid properties for the three different MR fluids and standard AFCO oil can be seen in **Table 1**.

Table 1: Typical Fluid Properties of Different MR Fluids (Lord 2011)

Fluid Name	MRF-122EG	MRF-132DG	MRF-140CG	Standard AFCO Oil
Appearance	Dark Grey Liquid	Dark Grey Liquid	Dark Grey Liquid	Clearish Gold
Viscosity [Pa-S @ 40°C]	0.042 ± 0.020	0.112 ± 0.020	0.280 ± 0.070	0.0915 (Based on SAE 5W Oil)
Density [g/cm^3]	2.28-2.48	2.95-3.15	3.54-3.74	N/A
Solids Content by Weight [%]	72	80.98	85.44	0
Flash Point [°C]	>150	>150	>150	N/A
Operating Temperature [°C]	-40 to +130	-40 to +130	-40 to +130	N/A

MR Fluid Application

The MR fluid from the Lord Corporation was chosen because Lord has been developing MR technologies since the early 1990's. Also their MR fluids were available in the time frame that was required. Since this thesis is evaluating how much benefit an MR damper gives over a passive damper, the two shocks should be similar when there is no magnetic field present. Therefore it was determined that the fluid should have a viscosity that was similar to that of the original factory oil which was roughly 0.0915 Pa-S @ 40°C. **Table 1** shows that the original oil

was between the MRF-122EG and MRF-132DG fluids. MRF-132DG was chosen because it was closer the original passive damper oil. Also with this fluid the maximum achievable damping force was greater due to the increase in the amount of iron particles suspended in the fluid. Having the highest achievable damping force without significantly changing the passive damping force of the MR fluid will allow for the two dampers to be evaluated effectively.

Magnetic Coil Theory

Magnetic coils produce a magnetic field within the bounds of the coil's length; A magnetic coil lends itself to an MR damper application, since a magnetic field is required inside the damper to control the MR fluid. In order for the magnetic coil to generate a magnetic field inside the damper tube, the coil has to be setup like the solenoid presented in **Figure 15**. The figure shows a long solenoid which is defined as having a coil length that is much greater than its radius (L>>r). **Figure 16** shows the approximate distribution of the magnetic field intensity along the length of the coil.

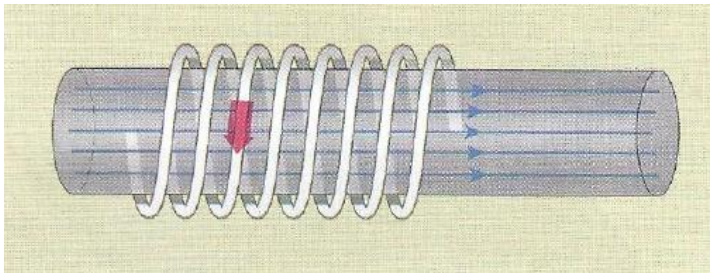

Figure 15: Long Solenoid (Reese 2000)

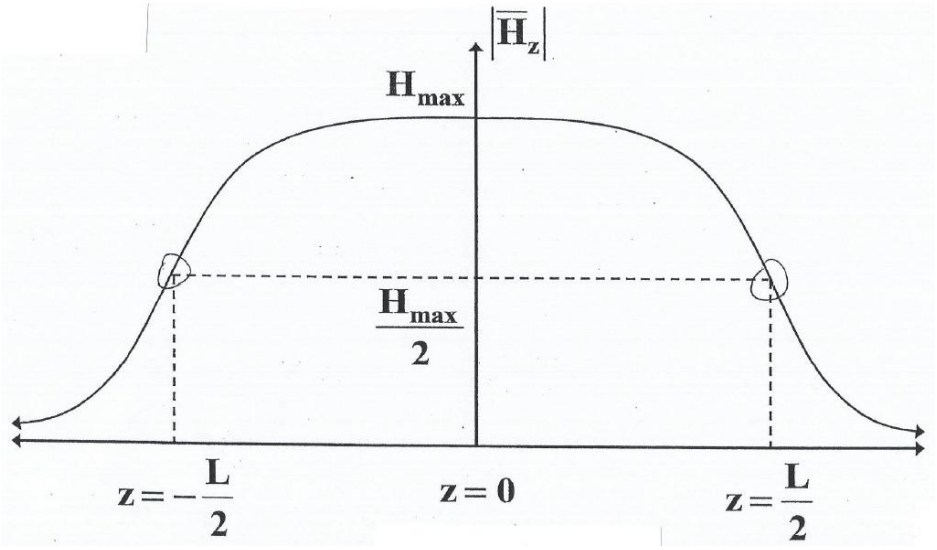

Figure 16: Approximate Magnetic Field Intensity Distribution (Gutschlag 2013)

The maximum magnetic field intensity will occur at the center of the coil. The derivation for the magnetic field intensity at the center of a long solenoid, $\overline{H}_{Center}$, is shown below (1) in terms of amps per meter.

$$\overline{H}_{Center} = \frac{N_{total} I \hat{a}_Z}{\sqrt{L^2 + 4r^2}} \cong \frac{N_{total} I \hat{a}_Z}{\sqrt{L^2}} \cong \frac{N_{total} I \hat{a}_Z}{L} \quad (For\ L \gg r) \quad (1)\ (Gutschlag\ 2013)$$

Where N_{total} is the number of turns; I is the current; $\hat{a}_Z$ is the unit vector; L is the length of the coil; and r is the radius of the coil. Also in the above figure it can be seen that the field intensity at the ends of the coil will be half of what it was at the middle of the coil. The derivation for the magnetic field intensity at the ends of a long solenoid, $\overline{H}_{Ends}$, is shown below (2) in terms of amps per meter. The same units apply as the above derivation.

$$\overline{H}_{Ends} = \frac{N_{total} I \hat{a}_Z}{2\sqrt{L^2 + 4r^2}} \cong \frac{N_{total} I \hat{a}_Z}{2\sqrt{L^2}} \cong \frac{N_{total} I \hat{a}_Z}{2L} \quad (For\ L \gg r) \quad (2)\ (Gutschlag\ 2013)$$

Based on the number of turns that was calculated in (1), more than one layer may be required to achieve the proper number of turns. The number of turns per layer, N_{layer}, is shown below (3).

$$N_{layer} = \frac{N_{total}}{L} \quad (3)$$

Once the number of turns per layer that could be achieved was determined, the number of layers required was calculated. The number of layers required was found using equation (4) below.

$$Required\ Layers = \frac{N_{total}}{N_{layer}} \quad (4)$$

The outer diameter of the coil, OD_{coil}, must be determined so that the other properties of the coil can be evaluated. This was accomplished by determining what the outer diameter of the center spool section, $OD_{spoolcenter}$, would be. Although the wire will pack into the gaps between turns when it is wound, it was assumed that the wire on one layer sits in line with the wire on the layer below it. This was assumed so that each layer thickness is the same as the diameter of the wire, D_{wire}. The equation for the coil outer diameter is shown below (5), in terms of inches.

$$OD_{coil} = OD_{spoolcenter} + 2(D_{wire} * Required\ Layers) \quad (5)$$

To determine the properties of the coil, the total length of wire required, L_{wire}, needed to be calculated using a standard circumference equation. The total length of wire was calculated in terms of feet. Every layer of wire is going to have a different diameter, so the diameter at the center of the coil, $D_{coilcenter}$, was used for the calculation of length because half of the turns were smaller and half were bigger. The coil center diameter was calculated in terms of inches. Since, the diameter is in terms of inches the total wire length was divided by twelve to achieve a length

in terms of feet. The equations, (6) and (7), for the diameter of the coil center and total length of wire for the coil, respectively, are shown below.

$$D_{coilcenter} = \left\{\left(\frac{OD_{coil}}{2}\right) - \left(\frac{OD_{spoolcenter}}{2}\right)\right\} + OD_{spoolcenter} \quad (6)$$

$$L_{wire} = \pi * \frac{D_{coilcenter}}{12} \quad (7)$$

The approximate weight and the wire resistivity are dependent on the length of wire and the wire gauge as can be seen below (8) and (9). For a given wire gauge the length per pound, L_{pound}, and the length per ohm, L_{ohm}, are approximated from the manufacturer. The approximate weight is in terms of pounds, lbs, and the wire resistivity is in terms of ohms, Ω.

$$Approx.Wire\ Weight = \frac{L_{coilcenter}}{L_{pound}} \quad (8)$$

$$Approx.Wire\ Resistivity = \frac{L_{coilcenter}}{L_{ohm}} \quad (9)$$

The voltage that the system required, $V_{required}$, was calculated using the wire's current rating and the approximate resistivity of the wire as shown below (10). Since the power source has a maximum voltage it can supply, the required voltage was needed in order to determine if any other components needed to be added to increase the available voltage.

$$V_{required} = Wire\ Current\ Rating * Approx.Wire\ Resistivity \quad (10)$$

The required power for the system, $P_{required}$, was calculated using the required voltage and the wire current rating as shown below (11). This was used to determine how much of the available power would be drawn by the coil.

$$P_{required} = V_{required} * Wire\ Current\ Rating \quad (11)$$

Magnetic Coil Design

Different coil placement designs were considered for the given application. Both internal and external placements were viable starting options. With the internal design, the coil could be smaller because the field didn't need to penetrate the damper body. The internal method would also not increase the external dimensions of the damper. This design would require a new piston to be created because the room required for the coil was not available in the passive damper piston. Also the connecting rod between the piston and the rod end would need to be redesigned to incorporate running the wires into the damper.

With an external design no modification to the inside of the damper would be needed. The external coil would have the wire wrapped around the outside of the damper body in some manner. There are a couple different ways of creating this external coil: wrapping the wire directly around the damper body or developing a holder to wrap the wire inside and putting the holder around the damper body. Wrapping the wire directly around the damper body has the added benefits of having one less piece to design and also one less source of weight for the system. Having the wire wrapped directly around the damper body will not keep the wire from moving around and unraveling. Although designing a holder to wrap the wire around adds some weight to the system, it allows for the coil to maintain its placement without unraveling or moving around. This makes designing a holder for the wire to be wrapped around a simpler and cleaner design option.

After looking at the different design options, the external coil design was chosen due to its simplicity. Since the piston inside the damper was set up in a way that didn't lend itself to having a coil inside it, a significant amount of modification would have been needed to include

an internal magnetic coil. The coil length was determined so that the majority of the stroke that the damper would travel was still within the bounds of the coil and the coil was still capable of being fit on the shock body without any modification. The inner coil diameter was set as 1.7" due to the constraints imposed by the shock body diameter; The diameter of the shock body was 1.5" with a spool wall thickness of 0.1." **Figures 17** shows the overall dimensions for the damper and spool.

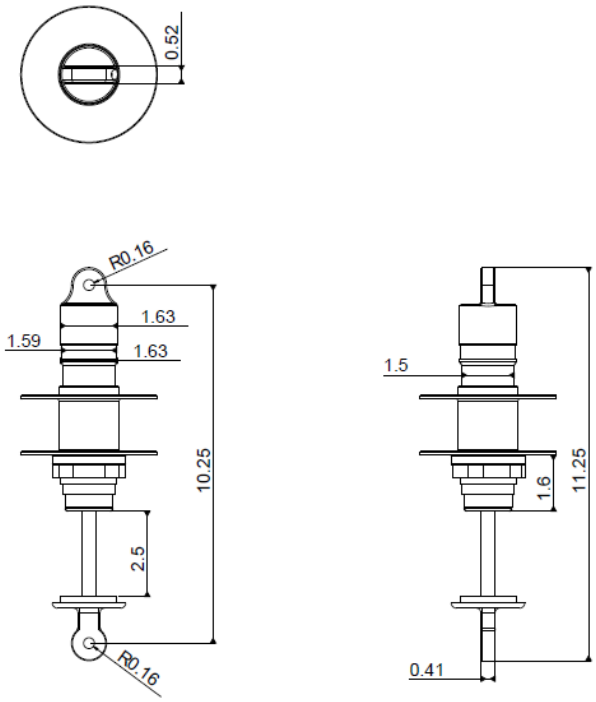

Figure 17: Prototype MR Damper Drawing (inches)

For use in this thesis, the coil for the MR damper was assumed to be a long solenoid because it was between that of a short solenoid and a long solenoid. By making this assumption the number of turns required is underestimated. Due to the dimensions being closer to a long solenoid though, the assumption estimates the number of coil turns closer than the short solenoid would. The coil had to be capable of being powered by the Formula SAE car's electrical system.

Also for use in this thesis, the above equations assume that the coil is wrapped around an air core. This assumption was made because the MR fluid permeability was not available from the manufacturer. The assumption causes the field strength to be underestimated because an air core has a lower permeability than that of the MR damper. The above equations, (1) and (2), showed that the current running through the coil is just as important to the field intensity as the number of turns. Since different gauges of wire will have different current ratings as well as a different number of turns that can be wrapped per layer, a few different gauges were considered. The wire had to be flexible enough that it could be wrapped without too much trouble, yet big enough so that the wire would be easy to handle during the winding process.

The required magnetic field intensity was needed in order to determine how many turns and the current required for the coil. It was decided that the desired field intensity should be 50 kAmps per meter. This will allow for the fluid to be controlled more simply because the range of yield stresses that the fluid will operate in is linear. The linear range can be seen in **Figure 18**. To produce a field intensity of this magnitude, the coil will need to be layered to reach the required number of turns. **Table 2** shows the coil properties for three of the different magnet wire gauges that were considered in the coil design. The different wire gauges of 16, 18, and 20 AWG required similar amounts of power to create the required field strength and they also produce similar coil diameters.

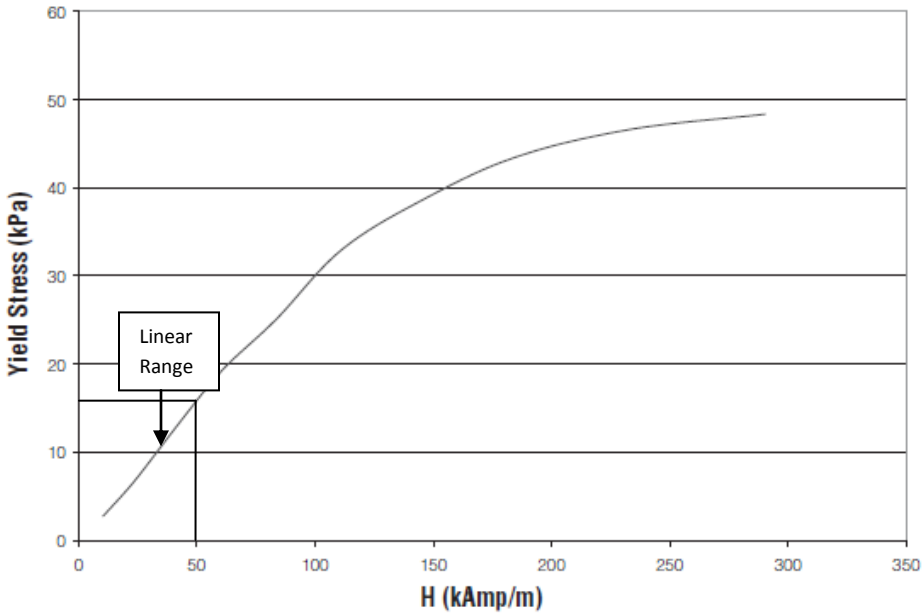

Figure 18: Magnetic Field Intensity vs. Fluid Yield Stress (Lord 2011)

Table 2: Coil Properties Based on Three Different Magnet Wire Gauges

Wire Gauge [AWG]	16 Gauge	18 Gauge	20 Gauge
Wire Rating [Amps]	3.7	2.4	1.5
L_{pound} [feet/pound]	125.6	220	314.6
L_{ohm} [feet/ohm]	249.004	156.617	98.522
D_{wire} [in]	0.0538	0.043	0.0346
N [turns]	515	794	1270
N_{layer}	28	35	44
Required Layers	19	23	30
OD_{coil} [in]	3.69	3.66	3.73
L_{wire} [ft]	363.06	556.59	902.23
Approx. Wire Weight [lbs]	2.891	2.5299	2.868
Approx. Wire Resistivity [Ω]	1.458	3.554	9.158
Required Voltage [Volts]	5.395	8.529	13.737
Power Required [Watts]	19.96	20.47	20.61

Keeping the current as low as possible was a consideration that was made in determining the proper gauge of wire for the application. Having a low current draw is important due to the limited power available in the Formula SAE car's system. The weight of the wire was an important consideration because the heavier the coil is, the smaller the benefit it will give to a lightweight vehicle. After determining the properties of the coil with different wires, 18 gauge

wire was chosen for the final design. It was chosen due to its ability to be easily wound around the coil spool and it also produced the lowest weight coil for the application. Due to the coil needing to be at least 23 layers thick, it was determined that high temperature wire was needed to ensure that the inside layers didn't overheat. Essex 18 AWG 200°C Rated High Temperature Magnet Wire was chosen for the application. The wire was wound around an outside spool as is shown in **Figure 19**.

Figure 19: Coil Prototype

Coil Spool Design

The magnetic coil had to be properly attached to the MR damper in order to minimize movement and also possibilities of damage. Instead of wrapping the magnetic coil around the damper body, the coil was wrapped around a spool. This allowed for the magnetic coil to be fit into the proper area without having the possibility of moving around or coming loose. The spool

was designed to fit snuggly around the damper body and use the spring preload nut to allow for adjustments to its placement along the dampers length. **Figure 20** shows how the spool was attached to the damper body. The placement of the magnetic coil on the damper's length allows for adjustments of which part of the stroke is affected by the magnetic field.

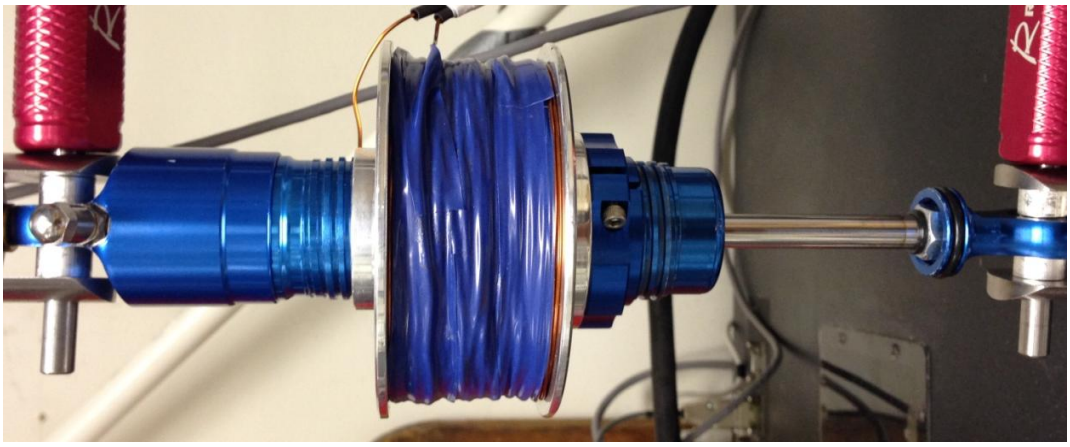

Figure 20: Spool Attachment

Since the magnetic coil diameter needed to be at least 3.66", the end caps on the spool were designed to be 3.9." This was done to ensure that the magnetic coil stayed within the confines of the spool ends. The overall length of the spool was designed to be 2.25" so all of the spring components could still be installed with spool on the damper body. To minimize the weight of the spool, the ends were made to smaller diameters. The bottom end touches the spring preload nut so the diameter at that end was made to sit flush against the nut without any overhang. The top end, on the other hand, was only touching the top portion of the damper the diameter was made to coincide with the diameter of the section the coil was wrapped around. By changing the diameter the only portions of the spool that had a diameter of 3.9" were the two 0.1" pieces setting the coil length. **Figure 21** shows the overall dimensions for the spool.

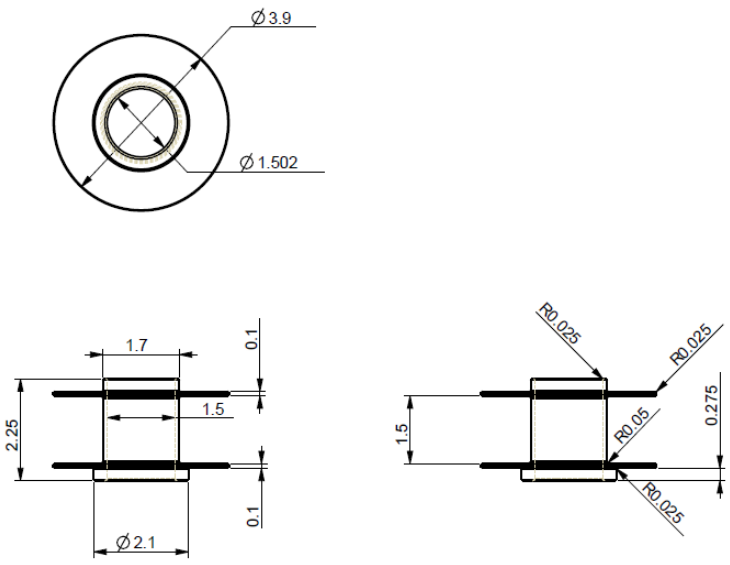

Figure 21: Spool Dimensions (inches)

Once the basic dimensions required for the coil were determined, an FEA was run in order to determine if a spool with the required dimensions would stand up to the different loads that it would be subjected to. During operation, the spool will be subjected to a number of different loading conditions. The first load is the pressure the magnetic coil will put on the center of the spool when it is tightly wrapped. For this loading case the wall of the spool's inner bore was fixed to simulate the spool fitting tightly against the damper body. The spool will also be subject to the magnetic coil pushing on the inside of the spool end caps. The center section of the spool was fixed for this case so that a pure bending scenario could be simulated at the spool end caps. The biggest component is the possibility of the spool end caps being impacted by an object. Everything except for the spool end cap was fixed so that none of the impact force was transmitted to other areas of the spool. **Figure 22** shows the loads applied to the spool. The material chosen for the spool was 6061-T6 Aluminum due to its high strength to weight ratio and ease of machining. The loads for the FEA were 25 pounds per square inch, 25 pound-force, and

100 pound-force respectively. **Figures 23** shows the results from the FEA with all the loads acting at once. The maximum stress of 3.042 ksi will occur at the inner section of the end cap, where it meets the center cylinder. The tensile yield strength for 6061-T6 Aluminum is 40 ksi and the ultimate tensile strength is 45 ksi (ASM). The yield and ultimate factors of safety were calculated as 13.149 and 14.793, respectively. It was determined from the FEA that the required dimensions for the spool were sufficient to withstand the loading conditions, so no further changes to the dimensions were needed. **Figure 24** shows the MR damper installed on the 2013 Bradley University Formula SAE car.

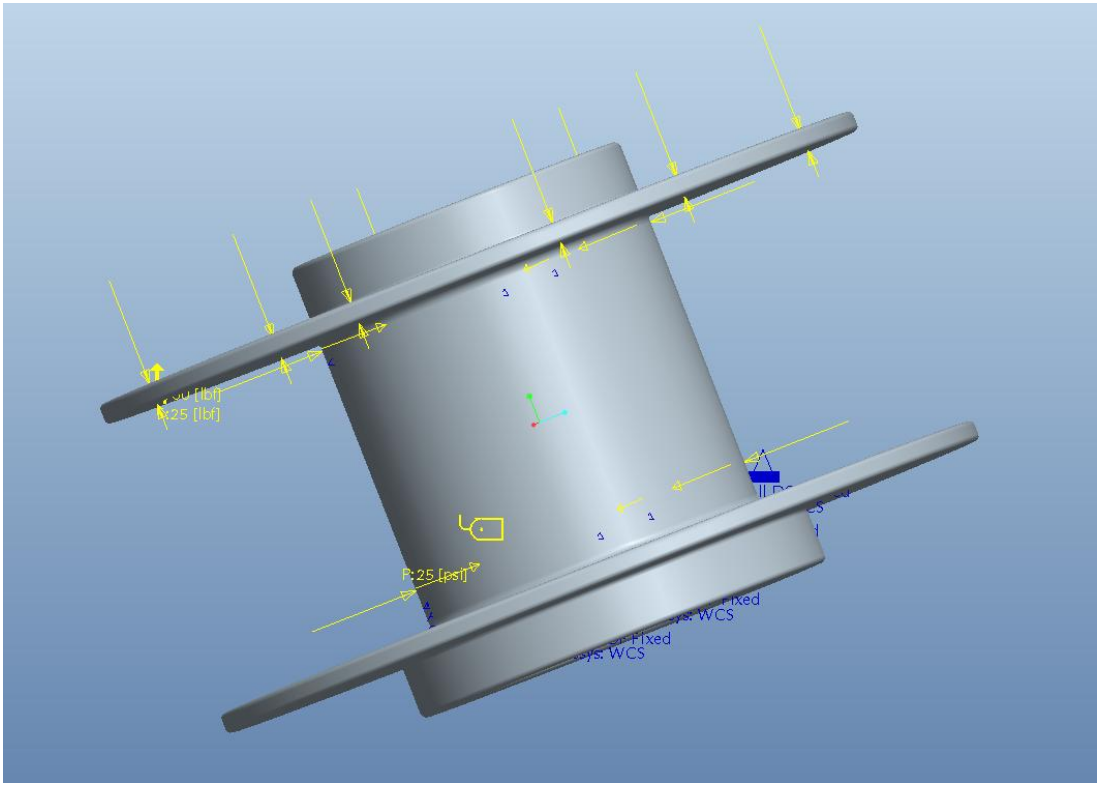

Figure 22: Loads and Constraints

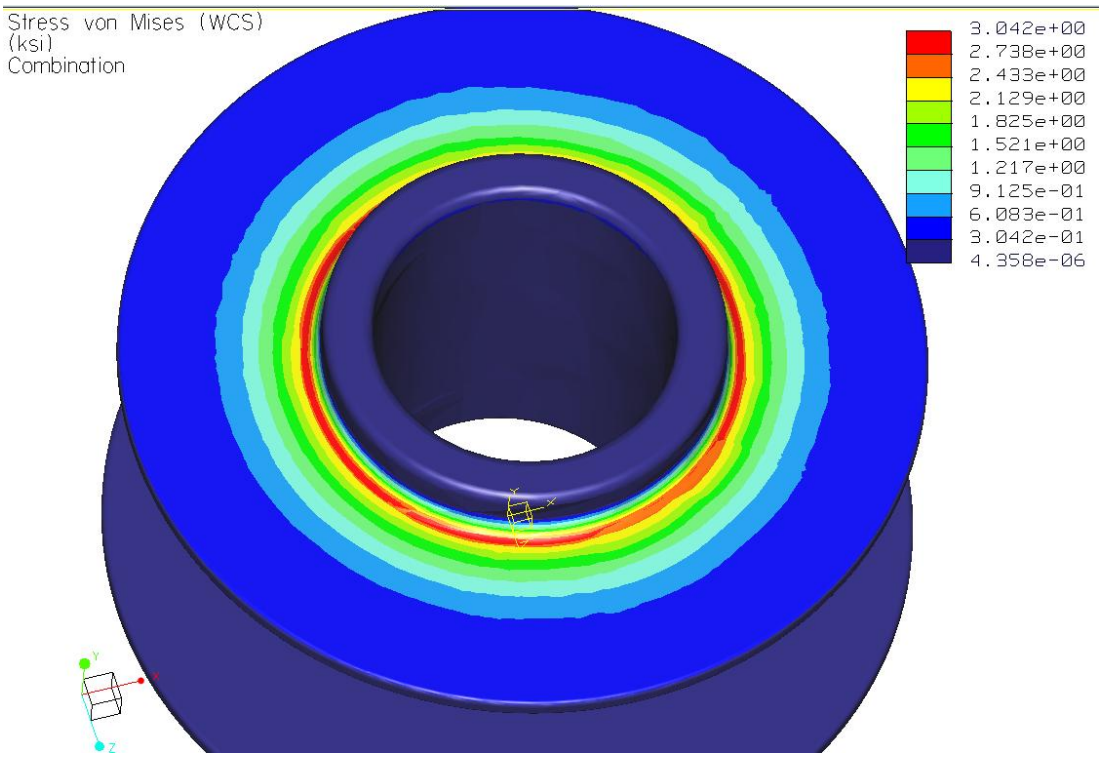

Figure 23: Top of Spool FEA

Figure 24: MR Damper Installed on Formula SAE Car

The model of the spool approximated the weight as 0.343 lbs and the final prototype weighed 0.338 lbs. The coil calculations approximated its weight as 2.5299 lbs with a total coil resistance of 3.554 Ω. The actual coil resistance was measured to be 3.6 Ω at the end of the extension wire and the wire weighed 2.522 lbs. The weight of the coil and spool together was approximated to be 2.873 lbs, and the final prototype weighed 2.86 lbs. With these values, the total length of wire was approximated to be 554.84 ft.

Chapter 3: Testing and Results

The MR damper must be tested in order to evaluate its damping characteristics. An MR damper's different curves are produced by varying current levels. Characteristics are typically represented by a force versus velocity graph called a damping curve. The main difference between an MR damper and a passive damper is the ability to have different damping curves. Determining these different damping curves, establishes the range of controllability that the MR damper can produce. Along with knowing the range that the MR damper operates in, the curves are used in developing a control strategy. In the control strategy, the curves are used to determine the proper current output to the magnetic coil.

Although determining the different damping curves is important, the most important aspect that needs to be tested is the performance of the system. In order to be considered as having satisfactory performance, the MR damper must produce consistent damping curves for a given current. The magnetic coil must also be able to withstand running at maximum current level for a continuous period of 10 minutes without overheating. Since the MR fluid starts to undergo plastic deformation once the effective yield stress has been reached, there is the possibility of seeing changes in the damping curve at a constant current if more cycles are run. These tests will evaluate the MR damper to experimentally determine its characteristics at different current levels.

Testing Apparatus

To achieve accurate and repeatable damping curves, the MR damper was tested in a controllable environment. Therefore, the MR damper was tested using the damper dynamometer. A Roehrig 2VS Damper Dynamometer with a 2 HP electric motor, shown in **Figure 25**, was used in all of the dynamometer testing. The dynamometer has the ability to produce 1250 pounds of peak force at 10 inches per second with a stroke length of 2 inches (Roehrig). The damping curves were collected with 3000 pound force sealed S-Type load cell from Interface Incorporated (Specifications in **Table 3**). The load cell was connected in series with the top clevis on the dynamometer to accurately measure the force that the MR damper was putting on the top clevis. This force is the same as the damping force that the fluid is putting on the piston inside the damper body.

The temperature of the damper and the magnetic coil is a concern when testing for the repeatability of an MR damper. To make sure temperature didn't influence the results, an infrared temperature sensor was used to monitor the damper temperatures. The infrared temperature sensor was produced by Raytek Corporation. The temperature sensor was attached to the left upright so that it had a direct line of sight to the MR damper body. The temperature sensor specifications are shown in **Table 4**. With these devices, the damping curves of the MR damper can be determined in a repeatable manner.

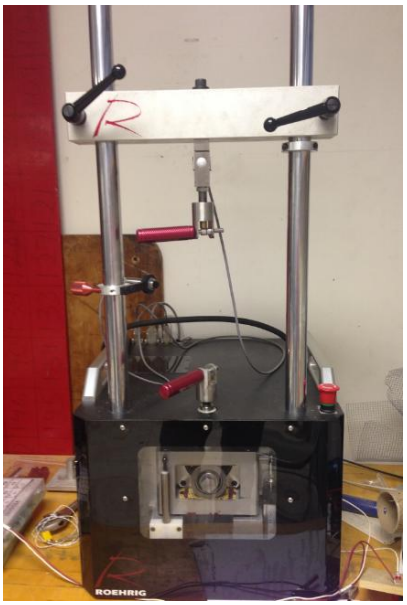

Figure 25: Roehrig Damper Dynamometer

Table 3: Interface SSM-AJ-3000 Load Cell Specifcations (Interface)

Max Excitation Voltage [VDC]	15
Rated Output [mV/V (Nominal)]	3
Nonlinearity [% FS]	± 0.05
Hysteresis [% FS]	± 0.03
Nonrepeatability [% FS]	± 0.02
Compensated Temperature Range [°F]	0 to 150
Operating Temperature Range [°F]	-65 to 200
Max Temperature Effect on Output [%/°F]	± 0.0008

Table 4: Raytek RAYCI3A Specifications (Raytek 2010)

Voltage Output Range [V]	0 to 5
Overall Temperature Range [°C]	0 to 350
Voltage Output [mV/°C]	10
Accuracy From 0°C to 115°C [°C]	± 3
Accuracy From 116°C to 225°C [%]	± 5
Accuracy From 226°C to 350°C [%]	>± 5
Spectral Response [microns]	7 to 18
System Repeatability	± 1% of measured value or ± 1°C, whichever is greater
Temperature Resolution [°C]	< 0.5
Response Time (95%) [mSec]	350
Emissivity	Fixed at 0.95
Optical Resolution @ 90% Energy	4:1

The optical resolution of the infrared temperature sensor is 4 to 1. Since an infrared temperature sensor takes an average temperature of the entire optical range, the proper distance between the sensor and the object being measured needs to be determined. **Figure 26** shows optical specifications for the infrared temperature sensor. To ensure that the magnetic coil temperature wasn't taken into the reading, the proper distance from the object to the sensor needed to be used. The area on the MR damper that was examined was the 1" area above the magnetic coil. The distance between the sensor and the damper was set to 4."

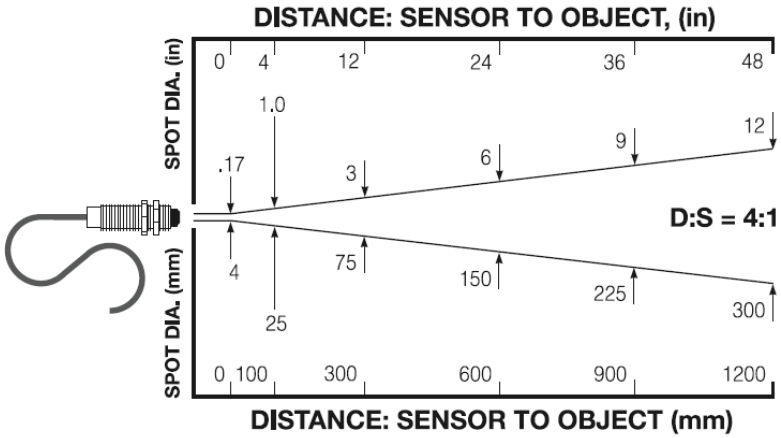

Figure 26: Raytek RAYCI3A Optical Specifications (Raytek 2010)

Damping Curves at Different Current Levels

In order to determine the feasibility of creating an MR damper out of a commercially available passive damper, a testing plan needed to be created. Different aspects of the MR damper will be tested to evaluate the overall feasibility of using an MR damper on an FSAE car. For each of the dynamic tests, a velocity of 8 inches per second was chosen. This velocity was chosen because the damper will be subjected to low speed (0-2 in/sec) and mid speed (2-8 in/sec) velocities while installed on a Formula SAE car.

To determine the damping curves that the MR damper can produce, a constant velocity plot (CVP) for the full damper cycle was produced. A CVP test collects data throughout the entire sine wave of the cycle. To test for the damping curves, a CVP test needed to be run for different currents. The maximum current that the MR damper was subjected to was 3.5 amps. Every half amp from 0 to 3.5 was tested to determine the full range of the damper. For all tests, the MR damper had a preload of 0.125" to ensure it didn't bottom out on the rebound stroke. The starting temperature for each test was set at 85°F to ensure that temperature didn't affect the damping curves. Knowing the maximum current and available damping curves will allow for the MR damper to be controlled more closely.

The MR damper was set up on the damper dynamometer before running any of the tests. The magnetic coil was positioned on top of the spring coilover nut for the tests. The bottom of the magnetic coil was positioned 1.6" from the bottom sealing plate on the damper body. Once everything was positioned, the MR damper was left in position for the entire set of tests to maintain the setup. After each test cycle the magnetic coil was turned off and both it and the MR damper were cooled to a room temperature of 70°F before starting the next test cycle. **Figure 27** shows the damping curves for 0A, 2A, and 3.5A. The entire range of damping curves that were produced in the test cycles are shown in **Figure 28**. The compression damping curve is above the x-axis and the rebound damping curve is below it.

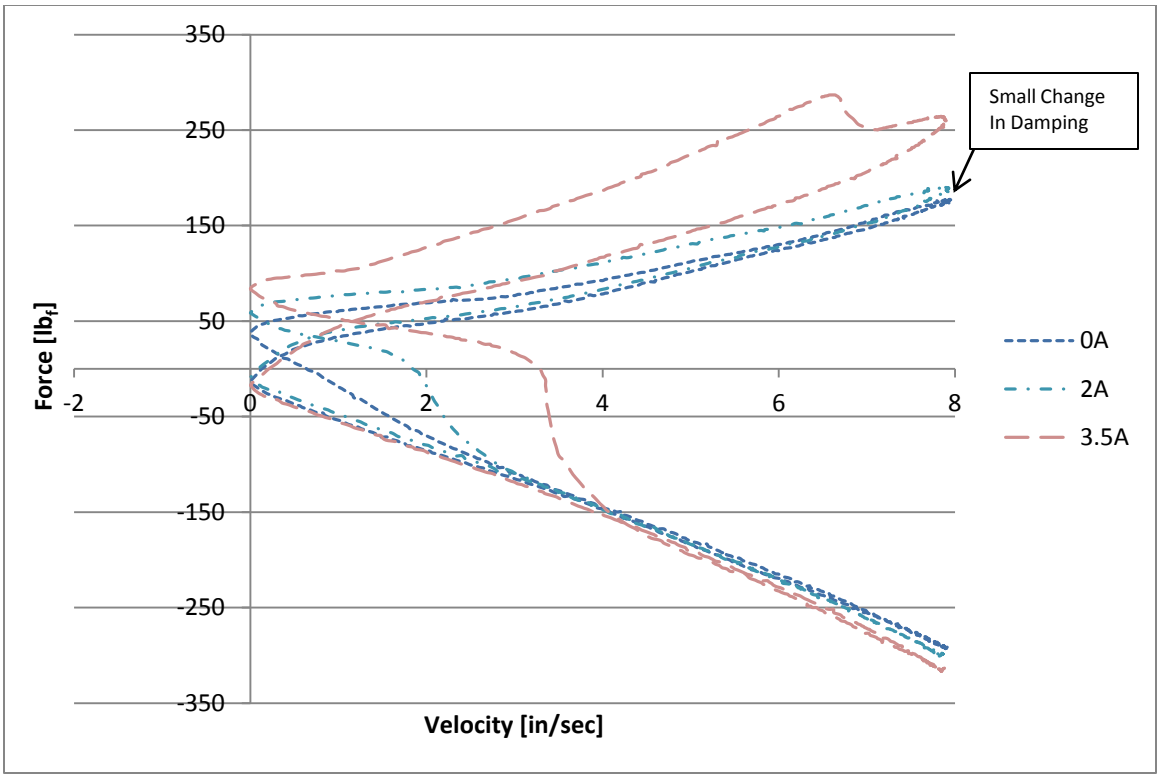

Figure 27: Damping Curves for 0A, 2A, and 3.5A

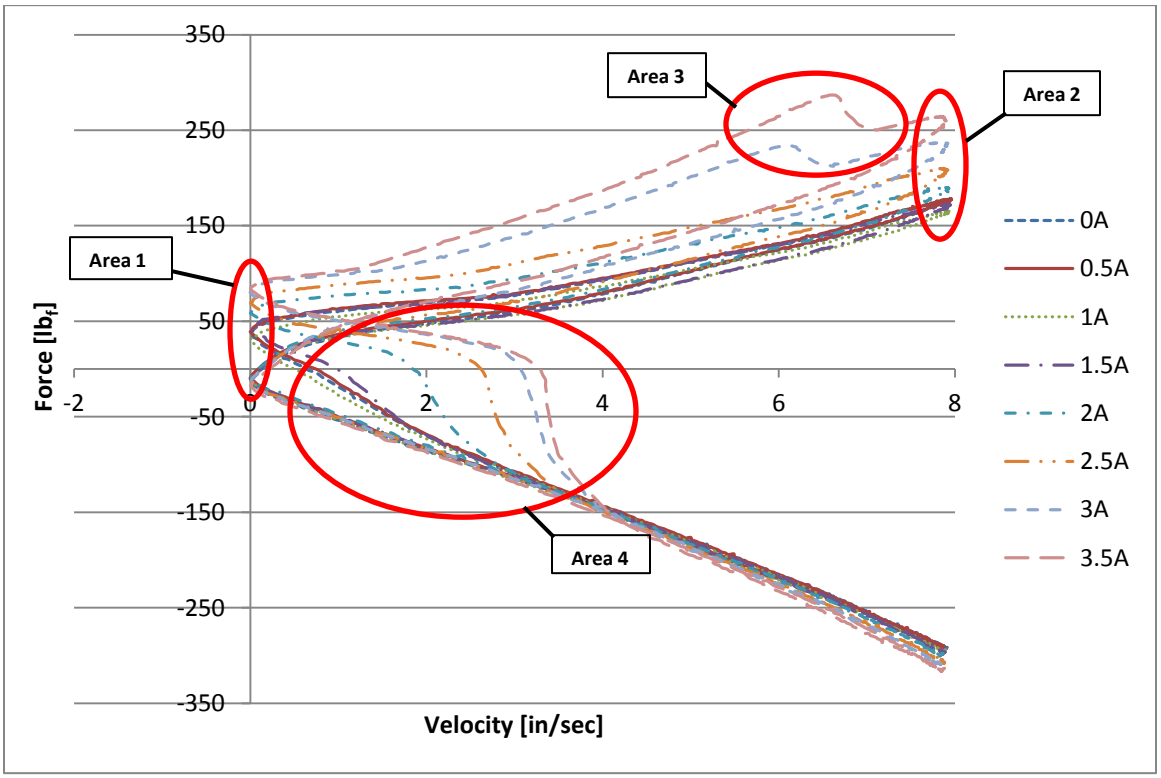

Figure 28: Damping Curves for Different Current Levels

The compression side of the damping curve steadily increases once the current reaches 2 amps, which is shown in **Figure 27**. At current levels lower than 2 amps, the damping curves stay relatively constant. This lack of change is due to the magnetic field strength being low enough that no significant change in the effective yield strength occurred. Below 2 amps the system doesn't produce any increases in damping. To produce increases in the damping, higher current levels need to be used. The system also requires more power at the higher current levels which draws more of the battery's available power. The force differences between when the piston is accelerating and decelerating become more significant as the current level is increased.

As the current increases so too does the hysteresis in the system, especially on the compression side. Area 1 shows that the point where the damper changes from compression to rebound shifts upward as the current increases. This area is a result of areas 2 and 3, where the hysteresis of the system originated. Areas 2 & 3 show the hysteresis of the different cycles as current increases. Area 2 specifically shows the transition from acceleration to deceleration of the compression stroke. Area 3 shows the change in hysteresis as the piston continues to decelerate during the compression stroke. The prototype MR damper therefore exhibits a modified Bouc-Wen hysteresis effect in the deceleration portion of the compression stroke. This phenomena accurately matches the model that was depicted in B.F. Spencer Jr.'s 1997 technical paper on the phenomenology of MR dampers. Which depicted that changes in the damping curves, hysteresis, occur due to the piston decelerating while the fluid flowing with the piston remains at a higher velocity. This in turn caused the damping forces on the deceleration side of the compression stroke to be higher than the forces on the acceleration side of the compression stroke. This can be accounted for in the control logic to make sure that the MR damper is accurately controlled throughout its stroke.

On the rebound side, there is very little change above four inches per second across the entire range of current levels. At the start of the rebound stroke there is a residual force due to the hysteresis in the MR damper which is shown by the area 4 of **Figure 28**. As the velocity increases, this residual force starts to dissipate until it reaches zero. Once the force reaches zero the damping curve develops a knee that causes the damping force to quickly increase until it reaches the true rebound damping curve. This occurred because the majority of the fluid that flowed through the piston during the rebound stroke was outside the bounds of the magnetic coil length. In a long solenoid the magnetic field stays within the bounds of the coil length, except for a very small amount of fringing that occurs at the ends.

Increasing Plastic Deformation Between Cycles

Although there has been substantial research into the effects that hysteresis and Bingham-plastic behavior has on the damping curve of an MR damper, cycle testing at a constant current has not been heavily researched. This poses an issue because if the current is held constant through a set of cycles, plastic deformation could increase causing cycle to cycle variance to occur in the damping curves.

Cycle to cycle variance is a controllability concern because a variance between cycles would introduce error into the system. This error would be related to the controller sending a voltage for a specific damping force and the system not responding with expected force. To look for variance between cycles, the MR damper was tested at a constant current for 5 cycles. The cycles were run one after another to ensure that the MR fluid had little time to change between runs. Also by running the test in this fashion, it simulates the affects of the damper actuating

multiple times in quick succession. A control group of cycles needs to also be tested at 0 amps to determine if the magnetic field is causing a variation between cycles. The variance can be accounted for through the testing and then included in the control strategy.

The current running through the magnetic coil was set at 3 amps for the entire group of cycles. As with the previous testing the damper was set with a preload of 0.125" to ensure the piston didn't bottom out during the test. The magnetic coil was again placed 1.6" up from the bottom sealing plate. The MR damper was at a room temperature of 70°F when the warm up stage of the test began. The damper was then allowed to warm up to 85°F before starting the testing. Once the test started, the magnetic coil was not turned off until the final cycle had finished. This was done to ensure that no changes to the MR fluid occurred as a result of change in magnetic field strength. The 0 amp control group was run first to determine a baseline and then the 3 amp group of cycles was run. **Figures 29 and 30** show the results from the 0 amp test and the 3 amp test, respectively.

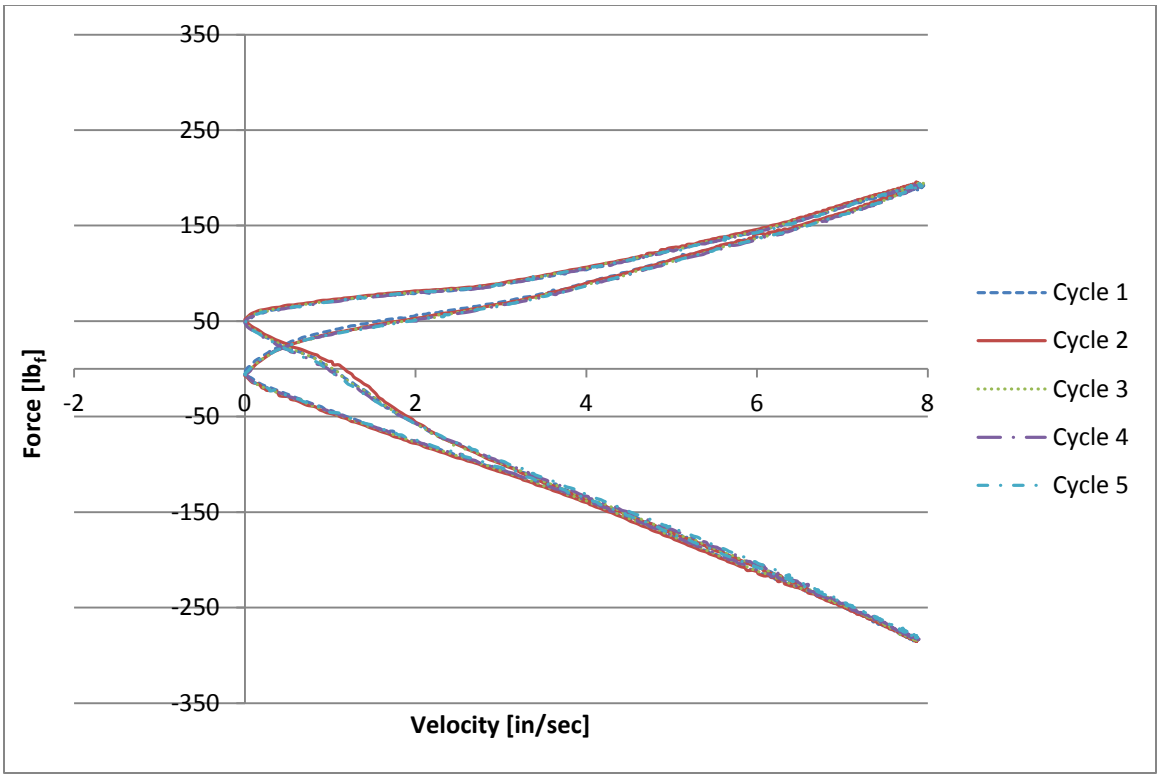

Figure 29: 5 Cycle Variance Test at 0A

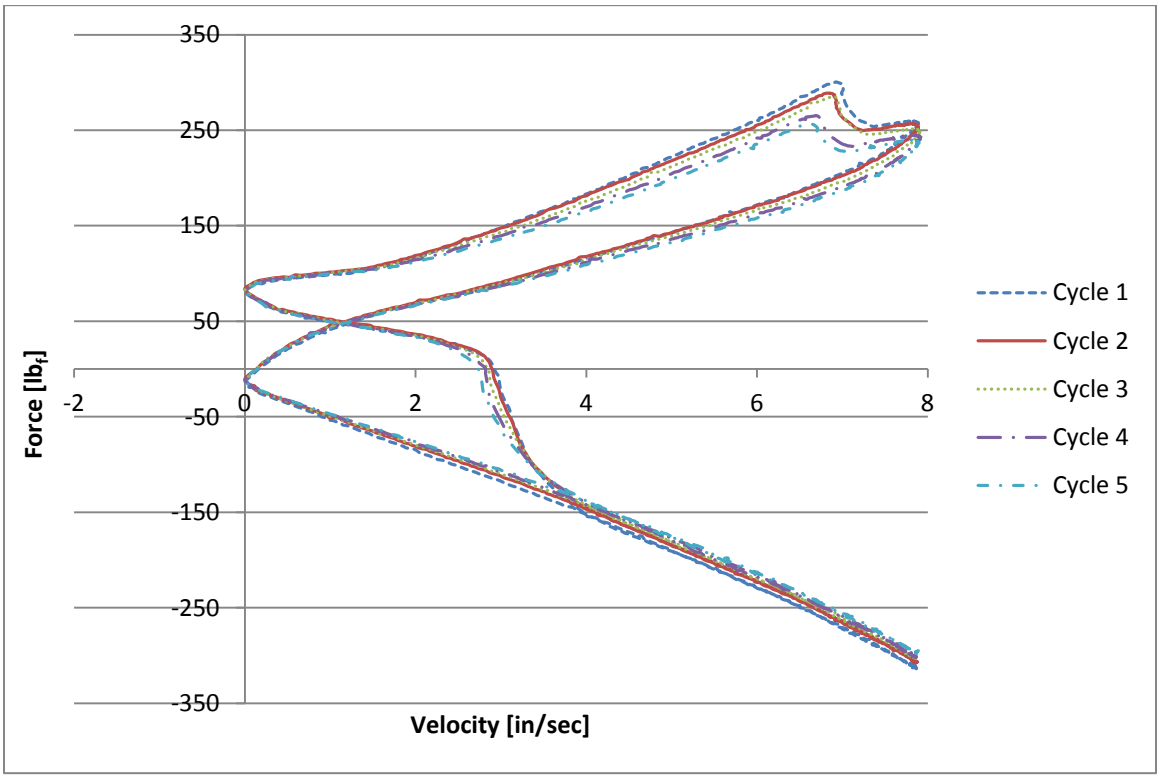

Figure 30: 5 Cycle Variance at 3A

The 0 amp test shows minimal variance from cycle to cycle, while the 3 amp test show significant variance. The cycle to cycle variance increases as the velocity increases. On the rebound side of the force versus velocity curve there is a very small amount of variance. Similar to the results that were shown in the test on damping curves at different current levels, the magnetic coil affects the variance on the compression side mostly. The variance between cycles becomes more pronounced above 2 inches per second. Since the tests were conducted without removing the MR damper or altering the setup, temperature and plastic deformation are the most likely causes for the variance shown.

To rule out temperature as a factor, two more tests at 3 amps were run. Each of the tests had 10 cycles run back to back in it. For the first test, the current running through the magnetic coil was turned off between cycles to allow for the MR fluid to reset itself. Between cycles there was a one and a half minute break to ensure that the MR fluid had a chance to return to its original state. By allowing the MR fluid to return to its original state, the goal was to prove that the variance was caused by continuing to plastically deform the semi-solid state. For the second test, the magnetic coil current level was kept at a constant 3 amps. To prove that plastic deformation caused the variance, the temperatures between the two test needed to be kept comparable.

To ensure this, the second test was also paused for one and a half minutes between cycles. This allowed for the temperature between tests to remain comparable for all the cycles. **Figure 31** shows the 1st and 10th cycle results for the first test where the current was turned off between cycles. The 1st and 10th cycle results for the second test where the current was left on throughout are shown in **Figure 32**.

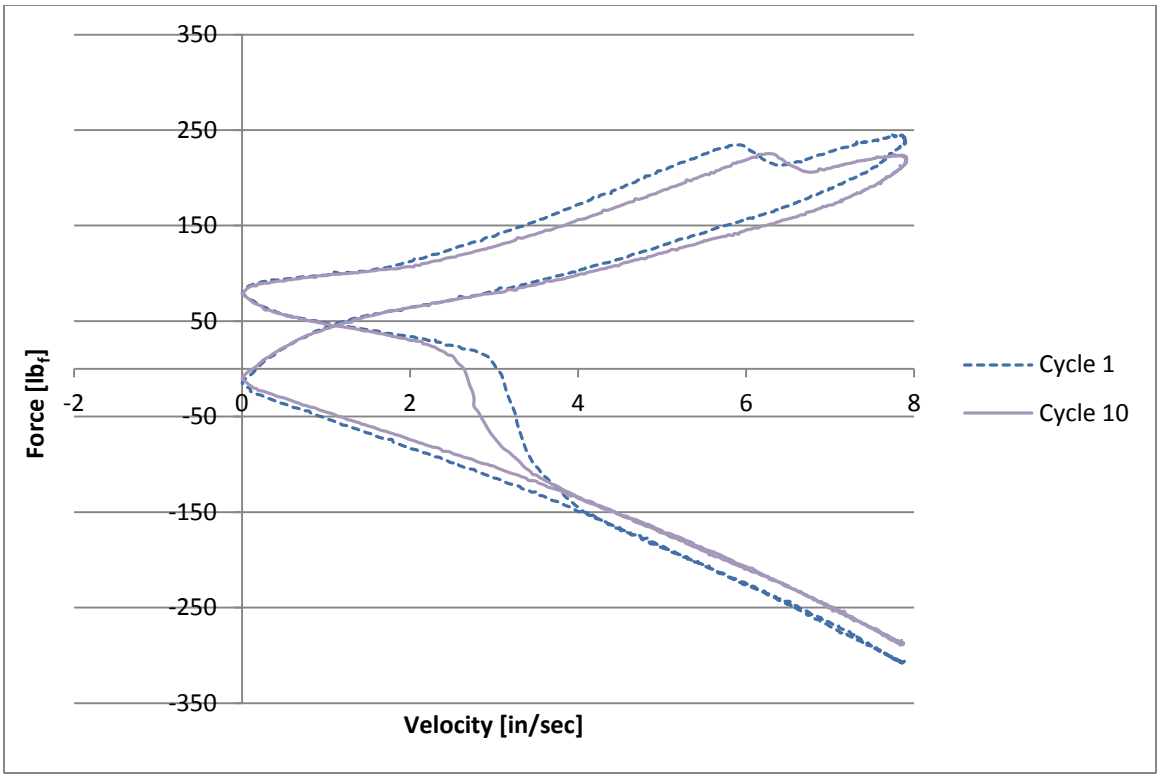

Figure 31: On/Off Cycle 1 vs. Cycle 10

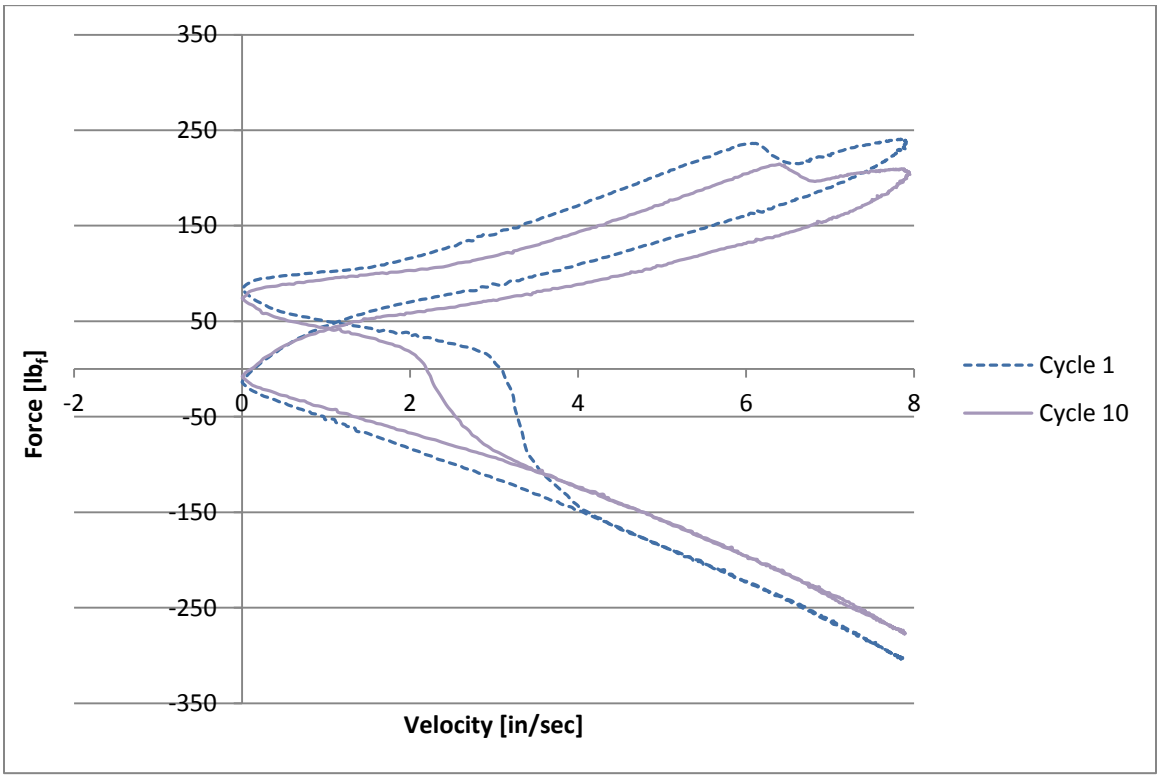

Figure 32: On Only Cycle 1 vs. Cycle 10

Both figures show signs of a variance between cycles. Although there is variance in both tests, the variance when the current is left on the whole time is much greater. The on/off test gave the MR fluid one and a half minutes to reset itself. Since the MR damper is not being actuated during this period the magnetic particles are no longer evenly dispersed. The time frame is not long enough for the fluid to settle so the chains that are created after the magnetic field is restarted are still different than the ones when the particles are dispersed evenly throughout the carrier fluid.

This plastic deformation causes the variance to occur as the cycles progress because more and more of the particles are pushed to the areas where they don't encounter the piston. The variance therefore is a direct result of the plastic deformation even when the magnetic field is dissipated for a short period of time without actuating the damper. **Figure 33** shows the relationship between the 1st cycle in both tests more clearly. The force versus velocity curves for the 1st cycles in both test relate closely to one another. The 1st cycle relationship proves that both tests started at roughly the same place. **Figure 34** shows the relationship for the total variation that occurred at the end of 10 cycles for each test. There is a significant variation between the 10th cycles in the two tests. **Table 5** shows the temperatures that were recorded at the start of each cycle.

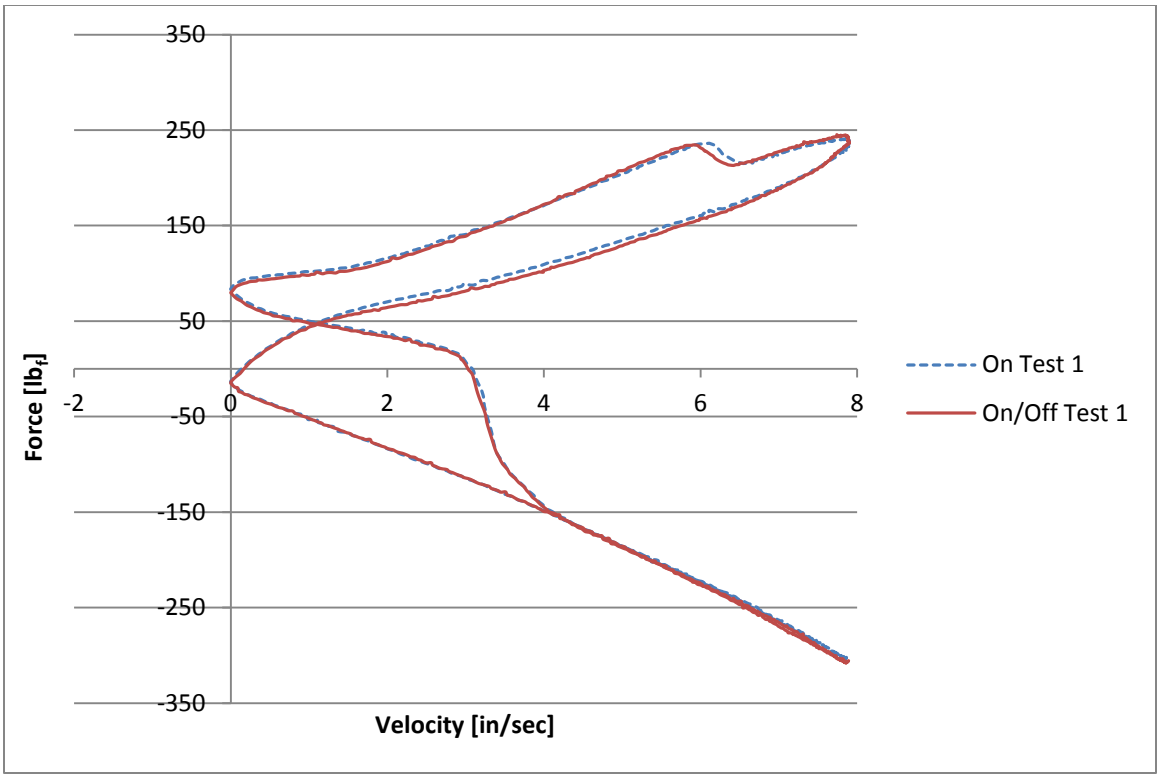

Figure 33: On Only 1st Cycle vs. On/Off 1st Cycle

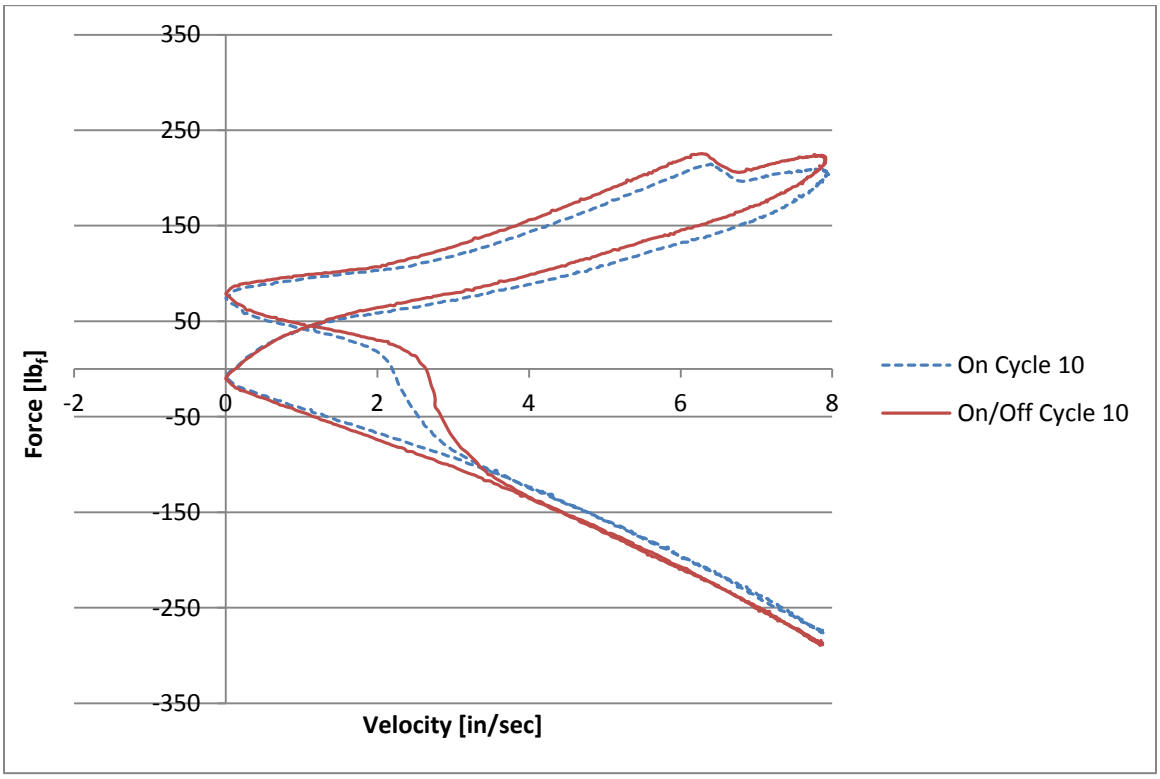

Figure 34: On Only 10th Cycle vs. On/Off 10th Cycle

Table 5: Cycle Temperatures for On/Off and On Tests

Test	On/Off [°F]	On [°F]	Difference [%]
1	85.28	86.14	0.998
2	88.96	90.04	1.199
3	92.53	93.69	1.238
4	95.80	97.01	1.247
5	98.87	100.33	1.455
6	101.75	103.50	1.691
7	104.69	106.45	1.653
8	107.47	109.40	1.764
9	110.02	112.30	2.030
10	112.04	115.05	2.616

By leaving the magnetic coil on for the entire test, the variation for 10 cycles is more significant. The temperatures start to increase faster as the cycles progress due to the magnetic coil heat soaking the MR damper. This occurs in the on test more than it does in the on/off test because the magnetic coil remains on the entire time. It can still be seen, that the two tests have closely related temperatures at adjacent cycles. Since the two tests had similar temperatures for the MR damper at each cycle, the temperature did not cause the variation between the 1st and 10th cycles. By not allowing the MR fluid any chance to reset itself, the plastic deformation continues to increase at a quicker rate in the second test. The plastic deformation also doesn't start to affect the damping curves until it reaches a velocity of 2 inches per second. This result is consistent with the other tests that were performed in this thesis since the shim stacks in the damper don't greatly affect the damping at velocities less than 2 inches per second. The plastic deformation can cause issues when the MR fluid is in a constant state of change. This makes it

more difficult to control the MR damper because the plastic deformation is different when the magnetic field intensity is left the same throughout a number of cycles versus changing the magnetic field intensity between cycles. The variance between cycles is caused by the plastic deformation in the MR fluid and is different depending on the setup of the MR damper.

Temperature of the Magnetic Coil

As current travels through the magnetic coil, it heats up the magnet wire due to the resistance in the wire. The magnet wire was rated for a temperature of 392°F before failure. To ensure no damage to the magnetic coil would occur under normal operating conditions, a durability test was performed. The magnetic coil was attached to the MR damper in order to use the infrared temperature sensor installed on the damper dynamometer. The maximum current level of 3.5 amps that the magnetic coil would be subjected to in operation was used for the durability test. This was chosen because operating at the maximum current load for an extended period of time would be the worst case scenario. Since most of the time the MR damper would not be running at a high current load, a period of ten minutes was chosen for the durability test.

This time frame was chosen to simulate running an entire Formula SAE autocross event at the maximum MR damper settings. To determine this, the magnetic coil was turned on while the MR damper was static and the temperature of the outside of the coil was recorded every ten seconds for the entire test. The centerline temperature sensor was adjusted to align with the center of the magnetic coil. Also, the distance from the coil to the sensor was set at 6" to allow for the temperature along the entire coil length to be read. The test was started when the magnetic coil was at a temperature of roughly 85°F. This temperature was chosen because all of

the other tests were started at the same temperature. **Figure 35** shows the temperature results for the durability test.

The temperature of the coil continues to increase with time, which was to be expected since the current remained constant throughout the test. The outside of the coil reached a temperature of 150°F after 10 minutes of continuous use. The wire in the center of the magnetic coil reaches the highest temperature but was unable to be measured accurately. By looking at the results for the temperature at the outside of the coil, it can be assumed that none of the wire in the magnetic coil reached the temperature limit. This is because the wire is wrapped around an aluminum coil spool which acts as a heat sink to draw heat away from the wire. The temperature of the spool was 200°F at the end of the test. Therefore even when the maximum current in maintained for an extended period of time, the magnetic coil doesn't encounter a temperature issue.

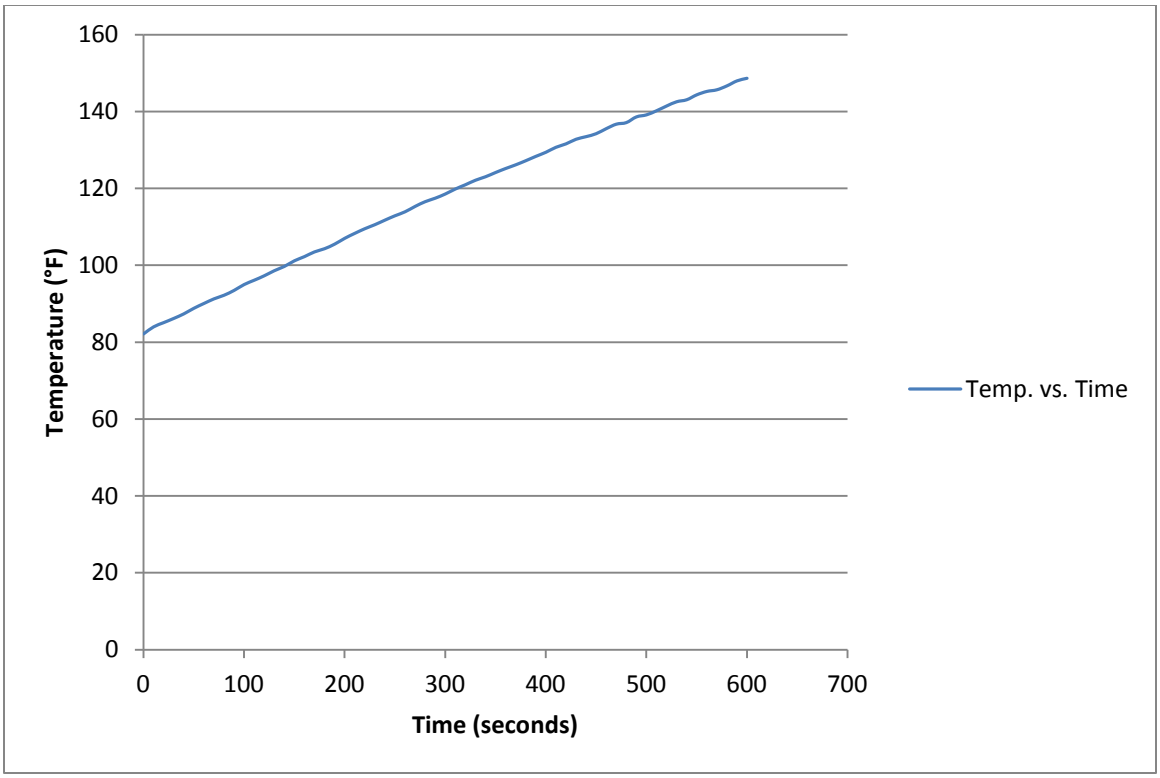

Figure 35: Magnetic Coil Temperature vs. Time at 3.5A

Testing on a Formula SAE Car

Until the MR damper has been tested on a Formula SAE car, it's feasibility can't be determined. The 2013 Bradley University Formula SAE Car was used to test the performance of the prototype MR damper. The prototype MR damper was installed on the front left corner of the car as shown in **Figure 36**. The front left corner was chosen because it had the most room for the MR damper and also because the type of maneuvers that were used in testing would transfer the most weight to the front outside wheel. The amount of displacement that the damper has directly relates to the amount of weight that has been transferred to the wheel attached to that damper. Since the objective of the MR damper is to reduce the amount of weight transferred to

the front outside wheel, the damper displacements need to measured. In order to measure the damper displacements, a data acquisition (DAQ) system and displacement sensors were needed.

The DAQ system chosen was and EVO3 Pro from AIM Sportline, which is shown in **Figure 37**. String potentiometers from Precision AutoResearch (PAR) with a travel of 15" were chosen for the displacement sensors. With the sensors being coupled to the DAQ system, an accurate damper displacement can be determined. The specifications for the 15" string potentiometers are shown in **Table 6**. With the setup described above, the performance of the MR damper on the Formula SAE car can be determined.

Figure 36: MR Damper Installed on a Formula SAE Car

Figure 37: EVO3 Pro DAQ System (AIM 2007)

Table 6: 15" String Potentiometer Specifications (Precision AutoResearch)

Input Impedance [Ω]	1000 ± 10%
Excitation Voltage [Max. Volts] (AC or DC)	25
Output Impedance [Ω]	0 to 1000
Linearity	± 0.5% of Full Scale
Operating Temperature [°C]	-15 to +60

Damper Displacement During a Skid-pad Maneuver

The maximum displacement of the MR damper during a constant radius maneuver will change as the damping force changes. This displacement will continue to change until the lateral acceleration of the car is sustained. To evaluate damper displacements for different settings, a skid-pad maneuver was performed. The skid-pad maneuver allowed for a lateral acceleration to be sustained, which put the MR damper into a quasi-static state. The changes to the MR damper displacement when it is in a quasi-static state will show whether the different setting has lowered the weight transfer to the front outside wheel. The skid-pad used in the testing has an inner diameter of 50' and an outer diameter of 70' with cones spaced out around both circles. This skid-pad layout mimics one half of the Formula SAE competition's layout (SAE 2013).

Three different settings for the MR damper were tested to evaluate their effects on the displacement that the MR damper had during the quasi-static portion of the maneuver. The MR damper was first set at 0A to show a baseline for the damper displacement with no applied magnetic field. To accomplish this, the system was unhooked from the battery to ensure no residual voltage made its way through the magnetic coil. The second setting was a midlevel one for the MR damper at 1.45A. This setting was used to show how the displacement changes at a low magnetic field strength. The last setting tried was 3.21A, which is close to the maximum

current the system is designed to use. This setting was used to determine how the damper's displacement is effected by a magnetic field strength close to the system's limit.

For all three tests, the skid-pad maneuver was performed in both directions. By performing the test in both directions, both the compression and rebound strokes can be studied for the MR damper. Also, to ensure that the driver does not play a role in the results, two different drivers with different driving backgrounds were used in the testing. Since the MR damper was installed on the front left corner of the Formula SAE car, right turns produce a damper in compression and left turns produce one in rebound.

The MR damper displacements at all three settings for when the MR damper was in compression are shown in **Figures 38 and 39**. For both drivers, the 0A and the 1.45A test produced sustained displacements of roughly the same amount. As was shown in **Figure 27**, the low current damping curves are roughly the same. Since the damping curves are about the same, it is be expected that the displacements of the two settings would be roughly the same. This data validates the results shown in **Figure 28** for the different damping curves. In both of the drivers tests at 3.21A, a significant difference in the sustained MR damper displacement is present. For both drivers, the sustained displacement was less than that of the other two tests. The goal of increasing the damping is to keep more weight on the other tires during the cornering maneuver. These results show that the amount of weight transferred to the front left tire was less than in the other two tests since the damper did not sustain as much displacement during the maneuver. The results show that the MR damper produces an increase in performance on the compression side when the current is at its high setting.

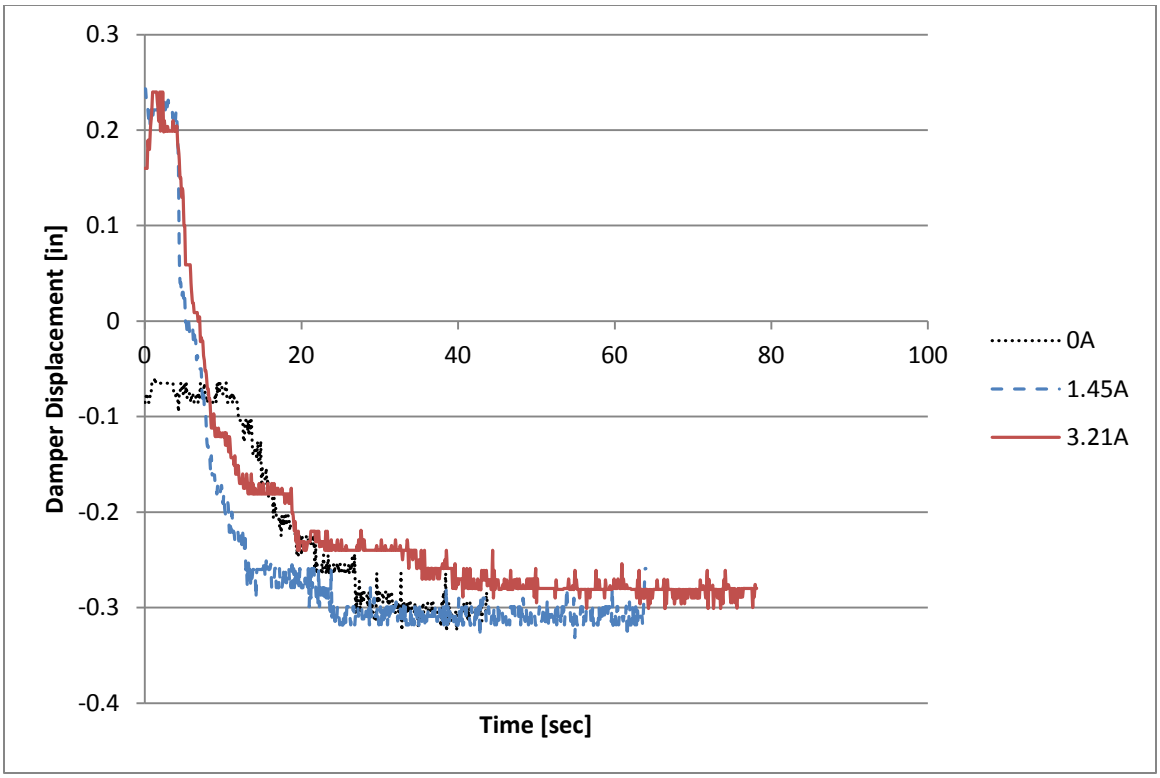

Figure 38: Right Turn Results for Driver 1

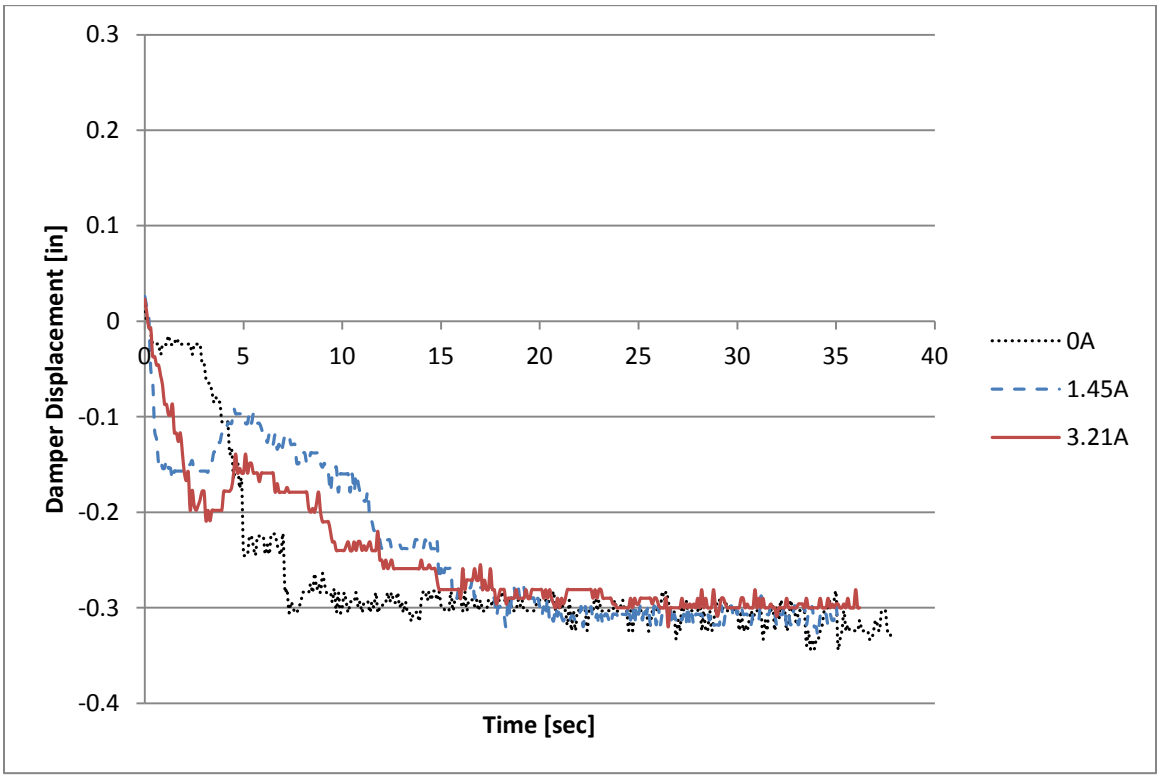

Figure 39: Right Turn Results for Driver 2

The displacement of the MR damper for all three current settings while it was in rebound are shown in **Figures 40 and 41**. The 0A and 1.45A settings while the MR damper was in rebound show the same phenomena as when it was in compression for both drivers. Both settings produce sustained displacements that are roughly the same as one another. During the 3.21A test, there was a decrease in sustained displacement for both drivers versus the other two settings. This is consistent with the testing from right turns where the MR damper was in compression as well. This shows that the front left corner where the MR damper was located, held onto more of the weight as the current was increased above 1.45A. This result is also consistent with the damping curves that were shown in **Figure 27**.

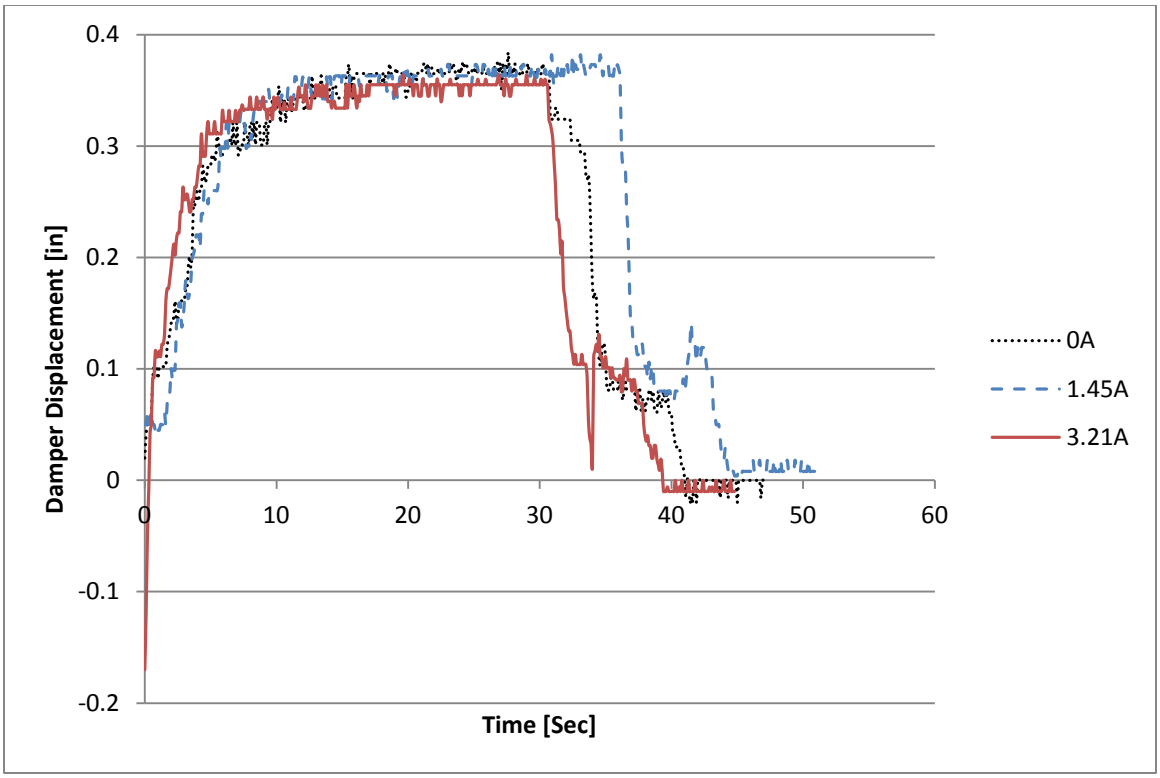

Figure 40: Left Turn Results for Driver 1

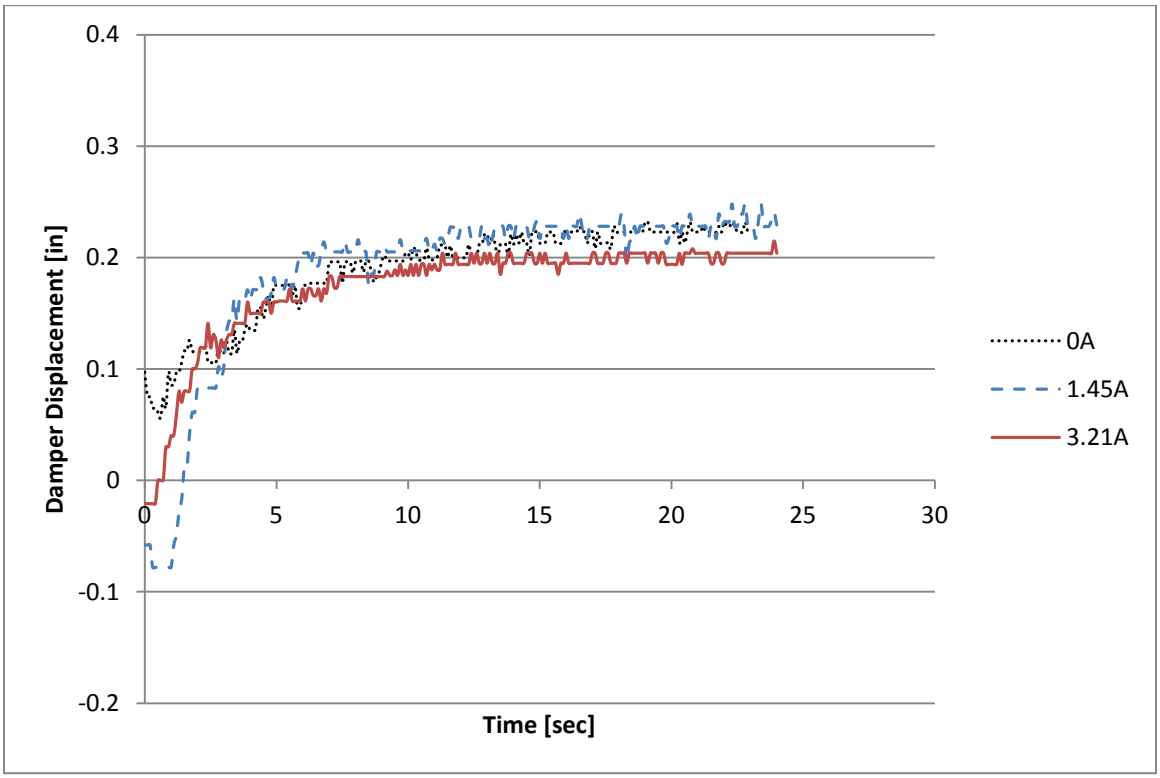

Figure 41: Left Turn Results for Driver 2

On the compression side, both drivers obtained MR damper sustained displacements of close to the same amount, but on the rebound side the sustained displacements were quite different. This difference was caused by an increase in the amount of weight transferred away from the rear left tire. During driver one's left turn testing, the rear left tire lifted off of the ground during the sustained lateral acceleration part of the test. When the rear left tire lifted off of the ground this caused all of the weight that was being put on it to be transferred to the other three tires. Although having the rear left tire come off of the ground is not beneficial, it did not play a part in the difference between the three setting because it occurred in all the left turn tests performed by driver one. The changes in the sustained displacement while performing right turns shows that the MR damper is performing in a beneficial manner for the Formula SAE car. The changes to the sustained displacement while performing left turns, is due to the increase in damping force that is associated with the increased rebound force that the MR damper achieves over the passive damper. To further determine if the MR damper is beneficial to left turns, a second MR damper must be installed on the other front corner of the car.

As the stability and predictability of the car increases, so too does the driver's confidence level. When the driver feels more confident, they can push the car further resulting in an increase in lateral acceleration. To evaluate this, two drivers performed similar slalom maneuvers to determine which setting helped to achieve the highest lateral acceleration. **Figures 42 and 43** show the lateral accelerations for the controlled slalom tests that were conducted at all three damper settings.

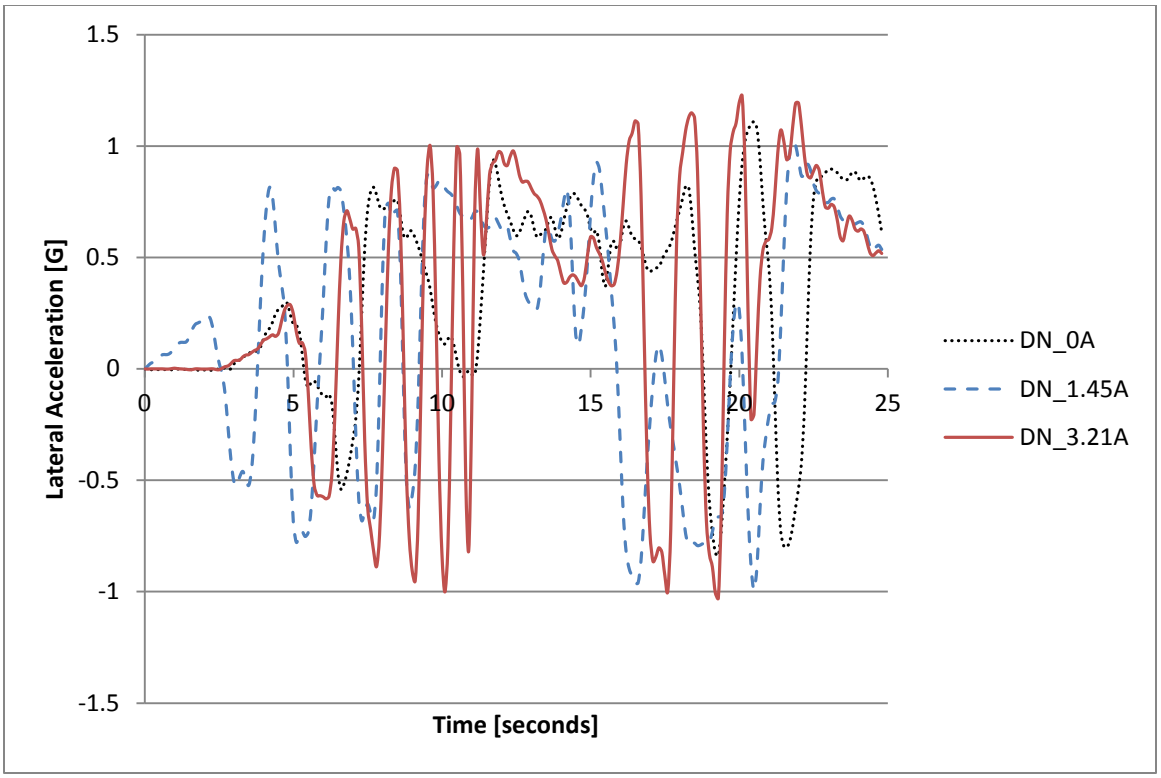

Figure 42: Slalom Results for Driver 1

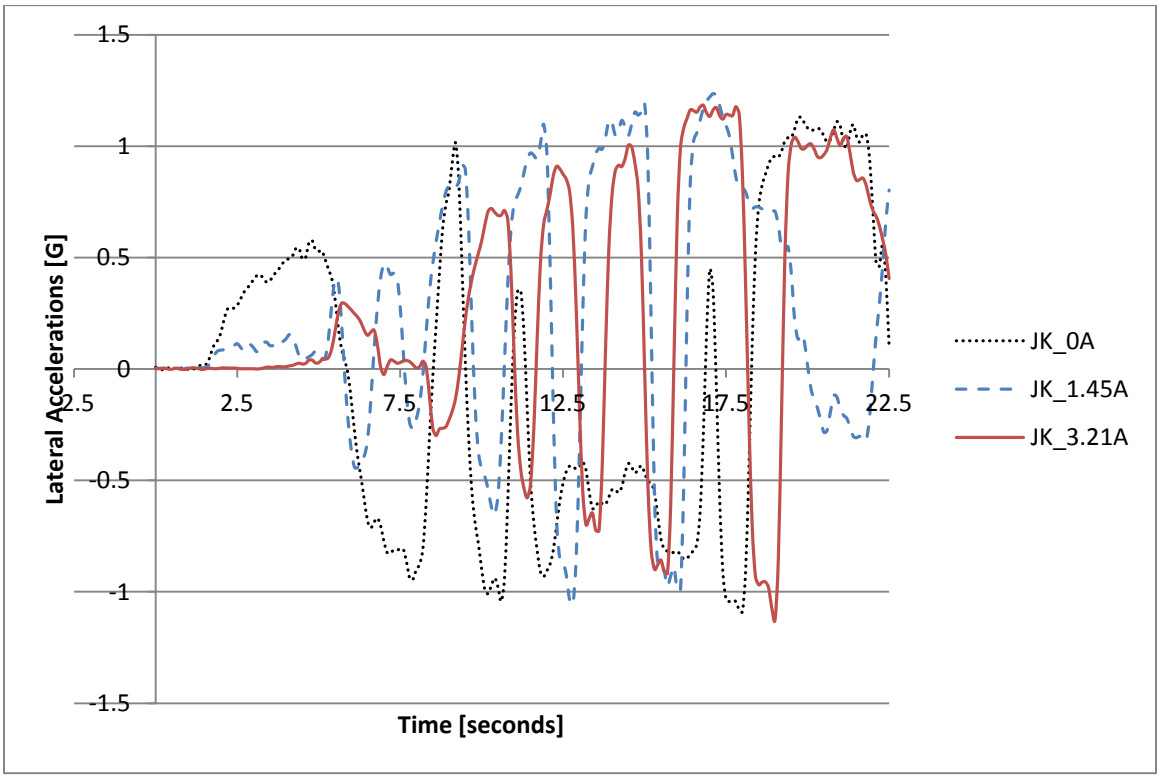

Figure 43: Slalom Results for Driver 2

Driver 1 achieved higher lateral accelerations in the slalom maneuvers when the MR damper was set at 3.21A. This increase can be attributed to the driver feeling more confident in the car as the current level was increased. For most of the test, driver 2 achieved similar lateral accelerations resulting from the damper being set at 1.45A and 3.21A. Towards the end of the slalom maneuvers though, driver 2 achieved the highest negative lateral acceleration when 3.21A was being used. The lateral acceleration results show that the driver was becoming more confident with the car, resulting in higher lateral accelerations as the test progressed.

Driver's Perspective on the Different MR Damper Settings

Although the data shows that the MR damper helps to maintain better grip by keeping some of the weight from transferring to the outside front tire while cornering, it is important to evaluate how the car felt to the drivers as well. The drivers can give insight on the car's behavior that is difficult to see in sensor data. For instance, if the car doesn't feel stable to the driver, that driver will be less likely to push the car to its limits. Therefore, driver input can significantly affect the resulting sensor readings. For these reasons, a driver debriefing session was conducted to determine both driver's perspectives on how the Formula SAE car handled during the different tests. For the 0A and 1.45A tests in both directions, the two drivers found that there was no perceivable change in the stability and predictability of the car between the two settings.

When the current level was increase to 3.21A though, both drivers felt that the car was more stable during sustained lateral acceleration maneuvers. They also felt that it was easier to predict how the car would react to different maneuvers. This increase in the perceived stability and predictability was found to be greater when the MR damper was in compression versus

being in rebound. This conclusion further validates the damping curves shown in **Figure 28** because there was not a strong increase in damping force on the rebound stroke. The increased stability and predictability was caused by the car having less tendency to oversteer or understeer. By having a car that was more neutral, the drivers likely made less severe corrections. To determine this, a twelve second timeframe for each of the three current levels during a skidpad was evaluated to determine the average lateral acceleration and the standard deviation of the results.

The twelve second timeframes for each of the three current levels for driver one are shown in **Figure 44**. The twelve second timeframe for driver two is shown in **Figure 45**. The lateral accelerations for the 3.21A current level are much more stable than the 0A and 1.45A ones for both drivers. This shows that by increasing the current level, the driver made less severe corrections. **Table 7** shows the driver one's results for the average lateral accelerations and standard deviations of the three different current levels. Driver two's results for standard deviations and average lateral accelerations of the three different current levels are shown in **Table 8**. The average lateral acceleration of 0A is less than the averages of the other two settings for driver one, while the other two settings produced values that were very close to one another. Driver two on the other hand, achieved roughly the same lateral accelerations for all three cases. This shows that driver two felt more comfortable in the car when no current was applied to the magnetic coil.

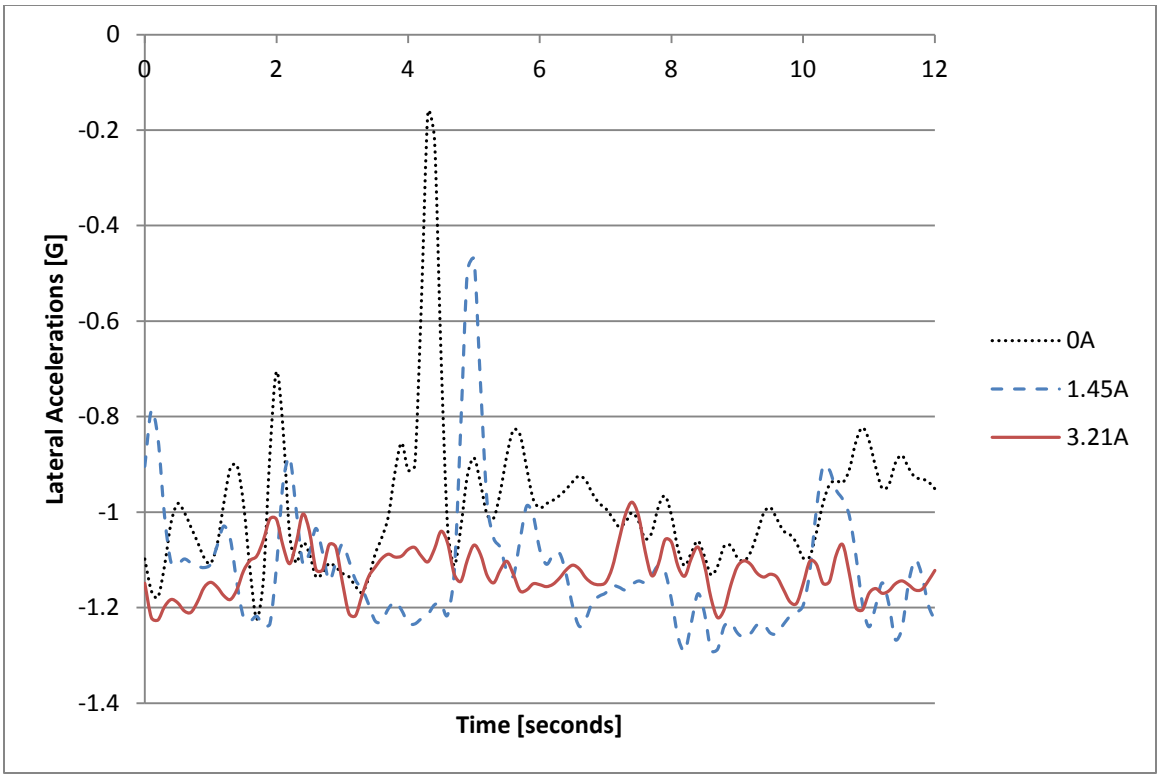

Figure 44: Continuous Right Turn Lateral Accelerations for Driver 1

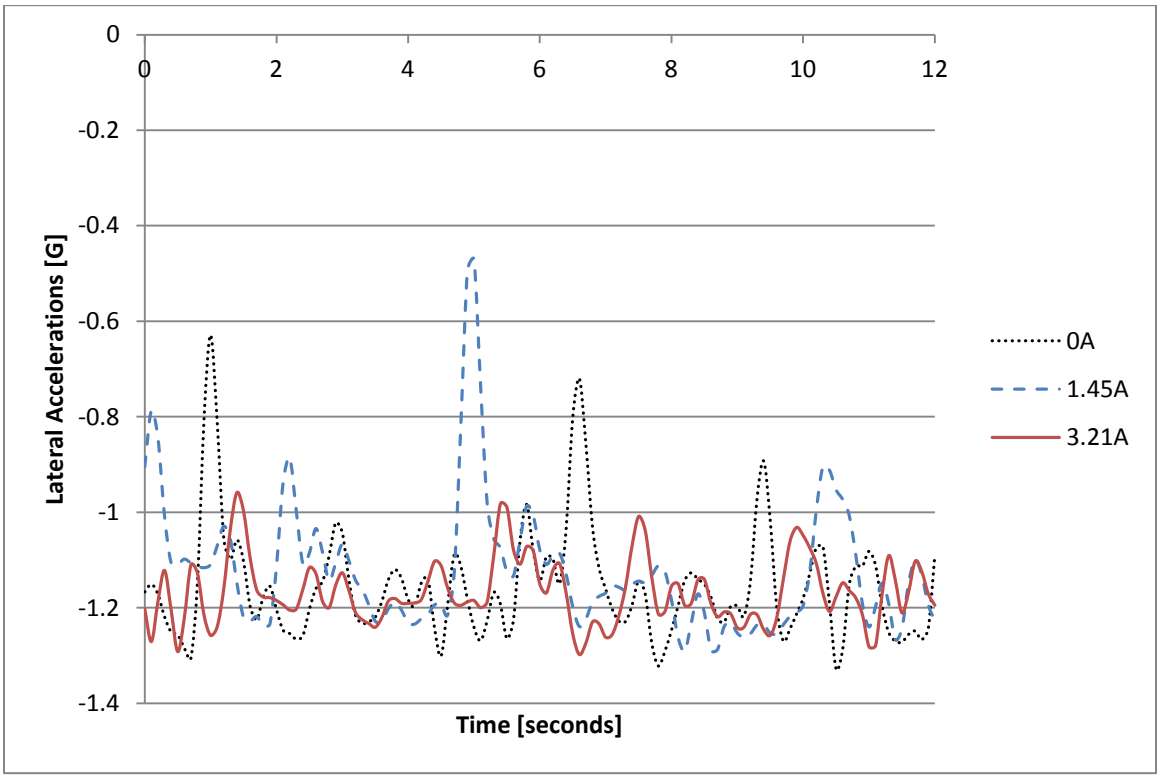

Figure 45: Continuous Right Turn Lateral Accelerations for Driver 2

Table 7: Right Turn Average Lateral Accelerations and Standard Deviations for Driver 1

	0A	1.45A	3.21A
Standard Deviation	0.147868	0.138094	0.051022
Average	-0.98768	-1.12173	-1.12606

Table 8: Right Turn Average Lateral Accelerations and Standard Deviations for Driver 2

	0A	1.45A	3.21A
Standard Deviation	0.118895	0.083407	0.068427
Average	-1.15436	-1.15226	-1.16739

Driver one's standard deviation between 0A and 1.45A didn't significantly change, but between 1.45A and 3.21A there was a substantial change. For driver two, the standard deviation consistently decreased for each of the different settings. This difference between the two drivers was attributed to differences in driving styles. These change in standard deviation from 0A to 3A show that the more neutral behavior of the car caused the drivers to make less severe corrections, hence their perception of the car as more stable and predictable during maneuvers. This perception allowed the drivers to push the car further because they felt more comfortable at higher lateral accelerations.

The driver perspectives show that the conclusions made from analyzing the sensor data, are also being seen in the cockpit. The MR damper helps to increase the stability and predictability of the Formula SAE car from a driver's perspective, which is caused by having better grip to all four tires. **Figures 42 and 43** showed that the driver's perceived increase in stability and predictability were caused by the change in current, which helped them to increase their lateral accelerations during the slalom maneuvers. Also, **Table 6** further backs up the driver's perspectives on the car and also validate that the MR damper is working in a beneficial manner not only to the performance of the car but to the driver as well.

Chapter 4: Conclusions and Recommendations

Conclusions

In this thesis, a prototype MR damper was developed from a commercially available passive suspension damper for use on a Formula SAE car. Testing on both the damper dynamometer and a Formula SAE car have proven that it is feasible to produce an MR damper for a small vehicle application out of a commercially available passive damper. The testing performed on the damper dynamometer proves that the MR damper changes significantly from current levels of 0A to 3.5A on the compression stroke. Testing on a Formula SAE car determined that the MR damper at 3.21A decreases the damper displacement, causing less weight to be transferred away from the inner two tires in a maneuver. This decrease in damper displacement proves that the MR damper benefits a Formula SAE car during cornering maneuvers. The testing performed with the MR damper installed on a Formula SAE car also showed that it increases the stability and predictability of the car at 3.21A. The prototype MR damper requires the use of MR fluid and a magnetic coil that is electrically charged from an external source.

The durability of running the magnetic coil at its maximum current for a period of ten minutes was also performed to determine if the magnetic coil could overheat during an extended period of use. Even with no forced convection, the magnetic coil failed to reach temperatures close to the limits of the magnet wire, proving that the coil will not have any issues with overheating during normal operating conditions. The hysteretic behavior of the MR damper was studied and the increase in plastic deformation due to continuous use was observed. The

increase in plastic deformation was postulated to be a result of continued cycles entering the plastic region while the magnetic field strength was held constant. It was concluded that by failing to allow the MR fluid any chance to reset itself after entering the plastic region, increases in the total plastic deformation occurred from cycle to cycle. These studies showed that allowing the MR fluid a chance to reset itself alleviates some of the plastic deformation associated with continuous cycling of the MR damper. Furthermore, it was shown that even when the MR fluid was given one and a half minutes to reset itself between cycles it was not enough to diminish all of the plastic deformation.

This phenomena was postulated to be due to the iron particles in the MR fluid not having sufficient time to settle back to their original location causing some residual plastic deformation to still exist. Producing an MR damper out of a commercially available passive damper for use on a Formula SAE car has been proven to be feasible. It has also been proven that there are significant benefits to using an MR damper on a Formula SAE car. It is concluded that the use of an MR damper on a Formula SAE car is a feasible option that should be consider when designing future cars for use in the Formula SAE competition.

Recommendations

Further development of the prototype MR damper would include refining the magnetic coil design to increase the magnetic field strength. This would give a broader range of damping curves to be produced, allowing for better use of the system at low current levels. Also, refining the placement and overall length of the magnetic coil to incorporate the rebound stroke better will help to give more controllability to the system. Further research into the plastic deformation

that occurs during continued cycling of the MR damper under a constant current should be conducted. This will help to further the understanding of how MR fluids behave when they are continuously subjected to plastic deformation. To further determine the feasibility of using an MR damper on a Formula SAE car, a basic control strategy needs to be developed to control a set of MR dampers installed on the front end of the car. A basic controller could use a string potentiometer to determine the direction the car is turning from the steering angle. With this steering angle, the controller could determine which damper is receiving the transfer of weight in a maneuver and increase the damping force to it. This will allow for more weight to be left on the other three tires which will help to increase overall grip of the car as well as stability and predictability that the driver feels in the cockpit. Developing a controller and control strategy for a pair of MR dampers attached to the front of a Formula SAE car would allow the system to be tested in many different situations. This type of testing is beneficial because the addition of two of these dampers and the extra battery and controller would not only negatively affect the competitor's cost event results, but would also add around ten pounds of sprung mass to the car. By researching this concept, the detriments of adding cost and weight to the Formula SAE car could be compared to the benefit that a semi-active suspension has in drivability.

References

1. "Aluminum 6061 ASM Material Data Sheet." *Aerospace Specification Metals Inc*., n.d. Web. 12 Sept. 2013.

2. AIM Sportline. *EVO3 Pista and EVO3 Pro User Manual*. Via Cavalcanti, Italy, 2007. Print.

3. Blanchard, E. "On the Control Aspects of Semiactive Suspensions for Automobile Applications." MS thesis. Virginia Polytechnic Institute and State University, 2003. Print

4. Bakaic, M. Personal Interview. 29 Nov. 2012

5. Choudhury, S. F., and M. Rashid Sarkar. "An Approach on Performance Comparison between Automotive Passive Suspension and Active Suspension System (PID Controller) using Matlab/Simulink." *Journal of Theoretical and Applied Information Technology* 43.2 (2012): 295-300. Web.

6. "Formula Student Combustion – World Rankings." *Formula Student Germany*, 17 Sept. 2013. Web. 19 Nov. 2013.

7. Guglielmino, E., et al. *Semi-Active Suspension Control*. London: Springer-Verlag London Limited, (2008). Print.

8. Gutschlag, S. Personal Interview. 17 Aug. 2013

9. "SSM/SSM2 Sealed S-Type Load Cell." *Interface Inc*., n.d. Web. 29 Oct. 2013.

10. Jawad, B., et al. "Controlling Weight Transfer with Active Damping." *SAE Technical Papers* (2007) Web.

11. Jawad, B., and J. Todd. "Effectively Approaching and Designing a Suspension with Active Damping." *SAE Technical Papers* (2002) Web.

12. Kasprzak, E. Personal Interview. 26 Nov. 2012

13. Komatsuzaki, T., et al. "Development of Electronically Controlled Shock Absorber using Magneto-Rheological Fluid." *SAE Technical Papers* (2007) Web.

14. Lacroix, B., P. Seers, and Z. Liu. "A Passive Nonlinear Damping Design for a Road Race Car Application." *SAE Technical Papers* (2006) *W*eb.

15. Li, W., et al. "Testing and Steady State Modeling of a Linear MR Damper Under Sinusoidal Loading." *Smart Materials and Structures* 9.1 (2000): 95-102. Web.

16. Lord Corporation. *MRF-132DG Magneto-Rheological Fluid*. Cary, NC., 2011. Print.

17. Marzbanrad, J., P. Poozesh, and M. Damroodi. "Improving Vehicle Ride Comfort using an Active and Semi-Active Controller in a Half-Car Model." *JVC/Journal of Vibration and Control* 19.9 (2013): 1357-77. Web.

18. Nabaglo, T. "Controller of Magneto-Rheological Semi-Active Car Suspension." *SAE Technical Papers* (2006) Web.

19. Poynor, J. "Innovative Designs for Magneto-Rheological Dampers." MS thesis. Virginia Polytechnic Institute and State University, 2001. Print

20. Precision AutoResearch. *LX-PA Series Sting Potentiometer*. Bensenville, IL., n.d. Print.

21. Raytek Corporation. *Raytek Compact Series Noncontact Temperature Measurement for Industrial Applications*. Santa Cruz, CA., 2010. Print.

22. Reader, D. "Nonlinear MR Model Inversion for Semi-Active Control Enhancement with Open-Loop Force Compensation." MS thesis. Virginia Polytechnic Institute and State University, 2009. Print.

23. Reese, R. *University Physics*. Pacific Grove, CA: Brooks/Cole, 2000. Print.

24. "2VS – 2hp – 1.5 kW Entry Level Damper Dyno." *Roehrig Engineering Inc*., n.d. Web. 29 Oct. 2013.

25. Society of Automotive Engineers International. *2013 Formula SAE Rules*. Troy, MI., 2013. Print.

26. Spencer Jr., B.F., et al. "Phenomenological Model for Magnetorheological Dampers." *Journal of Engineering Mechanics* 123.3 (1997): 230-238. Web.

27. Vetturi, D., et al. "Semi-Active Strategies for Racing Car Suspension Control." *SAE Technical Papers* (1996) Web.

28. Zhang, H., et al. "Skyhook-Based Semi-Active Control of Full-Vehicle Suspension with Magneto-Rheological Dampers." *Chinese Journal of Mechanical Engineering (English Edition)* 26.3 (2013): 498-505. Web